INTERNATIONAL ATOMIC ENERGY AGENCY
UNITED NATIONS EDUCATIONAL, SCIENTIFIC AND CULTURAL ORGANIZATION

INTERNATIONAL CENTRE FOR THEORETICAL PHYSICS
34100 TRIESTE (ITALY) - P.O.B. 586 - MIRAMARE - STRADA COSTIERA 11 - TELEPHONE: 2240-1
CABLE: CENTRATOM - TELEX 460392-1

H4.SMR.203 - 24

" SPRING COLLEGE ON GEOMAGNETISM AND AERONOMY "

(2 - 27 March 1987)

" The geomagnetic disturbances-definitions, physical meanings, handling and processing of data "

" The geomagnetic disturbances in high latitudes in relation with ionospheric parameters, field-aligned currents and aurora observations "

" Antarctic research: main tasks for studies in relation with observations in Arctic "

" The summary of geomagnetic disturbances studies: key parameters, practical results and future prospectives "

presented by :

A.N. ZAITZEV
Polar Geomagnetic Research Laboratory
Institute of Terrestrial Magnetism, Ionosphere and Radio Wave Propagation
(IZMIRAN)
142092 Troitsk, Moscow Region
U.S.S.R.

The geomagnetic disturbances-definitions, physical meanings, handling and processing of data.

A.N.Zaitzev, IZMIRAN

The magnetograms from ground-based level demonstrate various changes which are the manifestation of the processes on outer space. To-day we can assume that magnetic variations in physical sense consist of:

S+L+DP+DR+DCF+DT where

S - regular variation due to wave type emission of the sun; its statistical pattern - Sq- variation

L - regular variation due to lunar tides in the upper atmosphere

DP- irregular polar geomagnetic disturbances due to corpuscular type emission of the Sun (solar wind), its statistical pattern - S_D variation

DR- irregular variation due to the ring currents in the magnetosphere, which increases many times during global magnetic storms; its statistical pattern - main phase in Dst variation.

DCF-irregular variation due to currents on the magnetopause: its statistical pattern - initial phase of Dst variation

DT- the field of currents in the tail.

In this scheme some minor constituents are not included, because their impact in the variations on the ground-based level are negligible. The real impact of each component listed above strongly depends on period of day, season, latitudes and longitudes and previous conditions in the magnetosphere. The parts DP, DR, DCF and DT together organise the geomagnetic disturbance field.

The geomagnetic variations in terms of spectral properties presented in table 1. The natural geomagnetic variations have contirious spectrum and the band from 10 sec. to 10^5 sec. is occupied by geomagnetic disturbances.

In the Fig. 1 the concept of the magnetosphere is presented from which the position of the main sources of geomagnetic disturbances are evident.

On the Fig. 2 the concept of equivalent current system for auroral electrojet is presented. Note difference between the distribution of currents in evening hours, and two main features of current systems: current sheet and current electrojet.

Fig. 3 The results of statistical analysis of geomagnetic disturbances in the form of S_D variation for summer IGY.

Fig. 4 The horizontal component from auroral zone observatories for two substorms. Sharp negative bays are the main feature of substorms.

Fig. 5 The instantenious distribution of polar geomagnetic disturbances for the substorms demonstrated on Fig. 4. The position of electrojets presented by solid curves.

Fig. 6 Common-scale magnetograms for disturbed period december 19-20, 1980. From this magnetograms the definion of geomagnetic indexes are obvious.

Fig.7A The stocked magnetograms for the substorm of February 28, 1980 and B: latitude-time diagrams for separate components. The dynamics of substorm might be seen in details.

Fig.8A The stacked magnetograms for the substorm of May 28, 1979 as a sample with giant Ps6 pulsations. Bs the hodographs for different components for Ps6 event.

Fig. 9 LT-UT diagrams of AE-index for the period 17-18-19 March, 1978. Two types of substorms might be inferred from this diagrams: first, which is controlled by UT and second, which is controlled by LT.

Fig.10 LT-UT diagrammes of AE-index for period March 22, 1979 (CDAW-6). Note, that both substorms controlled by UT.

In this lecture we define the main sources of geomagnetic disturbances, physical meaning of geomagnetic indexes, we search the methods for handling and processing of data including the method of stacked magnetograms, instanteneous distribution of disturbance vectors, equivelent current systems, graphical displaying in form of latitude-time graphs, hodographs and LT-UT maps of AE-index.

The Biot-Savart law

The Biot-Savart law stated if we have linear current **I** located at the distance r from point of observations, the magnetic field $B = \frac{2I}{cr}$. The horizontal and vertical components for magnetic fied $H = \frac{2I}{c}\frac{h}{h^2+l^2} = \frac{Hoh^2}{(h^2+l^2)}$

$$Z = \frac{2I \cdot l}{c\cdot(h^2+l^2)} = Ho\,\frac{hl}{h^2+l^2} \qquad \text{where}$$

h - the heignt of current above the earth

ℓ - distance on the earth from projection of the current on surtace

In considering alternatives to the linear current interpretation of the magnetograms the current sheet of finite width must be ruled out. If we take the current model as a band with finite width and with uniform intensity across the band the components of the surface magnetic field at the distance ℓ from the axis of the band are:

$$H = \frac{I}{b}\tan^{-1}\frac{2bh}{h^2+l^2-b^2}$$

$$Z = \frac{I}{2b}\ln\frac{(l-b)^2+h^2}{(l+b)^2+h^2}$$

where 2b is the width of the band and I is the total current.

The Geomagnetic Disturbances in High Latitudes in relation with ionospheric parameters, field-aligned currents and aurora observations.

The main task for the study of the geomagnetic phenomena is attempt to infer the real electric current systems responsible for ground magnetic disturbances. Studies directed to examine physical processes occuring in the magnetosphere and ionosphere in terms of the growth and decay of the three-dimensional current system in the polar region which consists of ionospheric and field-aligned currents. Due to some uncertainties it is still not possible to construct the distribution of the three-dimensional currents without a number of assumptions. As a sample, we will discuss one of the methods proposed by Kamide, Richmond, and Matsushita, 1981.

On Fig.11 is presented a flow chart describing the important steps in KRM-method. After digitization and generation of orthogonal components in the chosen system of coordinates, we calculate the equivalent current function. This process involves fitting a magnetic potential function to the observed data and estimating the portion of this potential associated with overhead currents. The magnetic potential function V was represented by a spherical harmonic series in standard form:

$$V(\theta,\lambda) = \sum_{m=0}^{6}\sum_{n=m}^{56}(a_n^m \cos m\lambda + b_n^m \sin m\lambda)\cdot P_n^m(\cos\theta)$$ where

θ and λ are colatitude and east longitude in the eccentric dipole coordinate system, P_n^m - associated Legendre polynomials. The X_m and Y_m component at each station are expessedy by:

$$X_m = -\sum_m\sum_n (a_n^m \cos m\lambda + b_n^m \sin m\lambda)\,\frac{dP_n^m}{d\theta}$$

$$Y_m = -\sum_m\sum_n (a_n^m \sin m\lambda - b_n^m \sin m\lambda)\,\frac{P_n^m}{\sin\theta}$$

The computation was done at each grid point every 1° in colatitud and 15° (1hr) in longitude (local time).

It is then assumed that there is a relatively small and uniform internal contribution to the magnetic potential is extrapolated to 110 km altitude and converted to an equivalent ionospheric current function ψ by the standard procedure:

$$\psi_n = \frac{1}{\mu_o} \frac{2n+1}{n+1} \left(\frac{a}{R_E}\right)^n V_n^{(e)}$$

where $\psi = \sum \psi_n (\theta, \lambda)$, $a = R_E + 110$ km, $\mu_o = 4 \cdot 10^{-7}$ H/m.

On the Fig.12 the results of calculations are demonstrated in graphical form. After appropriate choice of ionospheric conductivity model we can calculate (or convert) such type of distribution in any related parameters as ionospheric currents and field-alighed currents.

If we assume that electrostatic potential $\Phi(\theta, \lambda) \approx F(\psi, 0,$ we can calculate the electric field $E = -$ grad Φ. Once the electric field is determined, the ionospheric current vector $\vec{I} = \Sigma_P \cdot \vec{E} + \Sigma_H \cdot \vec{E} \times \vec{n}_r$ where n_r is unit radial vector. From requirement that the three-dimensional current be divergence free,

$$j_{\parallel} = \text{div } I = \text{div } I_p$$

The height-integrated Joule heating rate is defined by $U_J = \vec{I} \cdot \vec{E} = \Sigma_P \cdot E^2$

On the Fig.12 we see ontput results in graphical forms. The modern computers can calculate such models in instantaneous manner, so we can present such calculation in the form of movie film. Next 6 minutes is movie demonstration, during wich we can see main features of dynamics in the high latitude geomagnetic disturbances.

Why we pay so great attention to field-aligned currents? Because they serve as a link between the processes in the magnetosphere and ionosphere and their dynamics closely related with physical processes in the magnetosphere. On the Fig. 13 we present a well-known scheme of FAC distribution according Iijima and Potemra, 1976. The main features of this scheme as follows: the currents are concentrated in two belts, which encircle the geomagnetic pole; region 1 located at the poleward side, region 2 located at the equatorward side. The region 1 currents flow into the morning sector and away from the ionosphere in the evening sector. The region 2 currents flow in the opposite direction at any given local time. These currents are closely associated with ionospheric currents, convection electric fields, auroral emissions and plasma instabilities. Now we can divide the field-aligned currents in terms of its scale: large--scale and small-scale. The main features of FAC summirized in Appendix 2.

The ground-based geomagnetic disturbances and FAC are closely connected with aurora, i.e. aurora events are the visible manifestation of processes in the magnetospheric sudstorms. On the next few slides are demonstrated the colorful pictures of aurora from which two basic types of aurora evident: active, sporadic and diffuse auroras. As was shown by simple calculations only few percent of incoming flux particles energy realised in auroras so close spatial correlations in the structure of auroras and geomagnetic disturbances is not always observed. Large-scale features follows each other very well, small-scale features have many discrepancies. On the next Fig. 14 is shown the developmen of aurora substorm according Y.Feldstein and G.Starkov. The auror distributed along auroral oval and main features of the oval relate with the structure of magnetosphere. With improvments of technique of aurora observations give us the new possibility for studies. Introducing the TV-devices led to new conclusions about structure of aurora displays. It was found that practically every aurora form has own structure and small-scale irregularitie are the main feature of every aurora event. On Fig. 15 presented reluts of small-scale observations of aurora by TV-method accordi T.Oguti, which are in close agreement with previous large-scale oval pattern.

Other methods for study the interrelations between auroras and magnetic disturbances are the satellite measurements. There are two types-measurements of particles and fields and auroral images On the Fig. 16 presented sample of measurements from ISIS-2 satellite. It shows main features of auroral particle precipitations in relation with geomagnetic disturbances in auroral zone

Most spectacular observations of aurora as made by aurora imager installed on satellites. On the next few slides demonstrated illustrative results from DE-1. During 1986 comparitive results was obtain by VIKING satellite. The intensive development of satellite imagers will lead to new level of knowledge about aurora dynamics and its relation with magnetospheric substorm processes.

In this lecture we examine the quantitative methods of analysis for geomagnetic disturbances on the ground-based level, the sequence of observations with field-aligned currents and interrelationship between geomagnetic disturbances and auroras which monitored on the ground-based level and on the satellites.

FIELD-ALIGNED (BIRKELAND) CURRENTS

The importance of "Birkeland currents" to the coupling between the magnetosphere and the polar ionosphere is emphasized by their intensity, which ranges between 10^6 and 10^7 amperes, and by the energy which they dissipate in the upper atmosphere, which can exceed by a considerable factor the energy dissipated there by auroral particles. The large- and small-scale average properties of field-aligned currents, determined from spacecraft observations, are summarised here. The density and flow direction of Birkeland currents associated with magnetic disturbances, ΔB, are determined from the relationship

$$J = \frac{1}{\mu_0} \nabla \times \Delta B.$$

The magnetic disturbances associated with Birkeland currents occur predominantly in the geomagnetic east-west direction (B_y) so that

$$J_{\parallel} = J_z = \frac{1}{\mu_0} \frac{\partial}{\partial x} B_y,$$

where x is directed toward the north, y toward the east, and z is positive downward and parallel to the main geomagnetic field. This formulation also presumes that the Birkeland current sheet is uniform in the east-west (y) direction; (i.e., the Birkeland current sheets are aligned in the east-west direction and are "infinite").

Since $\mu_0 = 4\pi \times 10^{-7}$ henry/meter,

$$J_{\parallel} = 8 \times 10^{-4} \frac{\partial B_y}{\partial x} \ A/m^2,$$

where B_y is in nanoteslas (nT) and x is in meters.

Since the speed of low altitude satellites like TRIAD and HILAT is approximately 8 km/second,

$$J_{\parallel} = \frac{1}{\mu_0} \left(\frac{\partial x}{\partial t}\right)^{-1} \frac{\partial B_y}{\partial t} = 0.1 \frac{B_y}{t} \ \mu A/m^2,$$

where $\partial B_y / \partial t$ is in nT per second.

A 200 nT gradient over a 160 km distance (covered in 20 sec by a low altitude satellite) corresponds to a typical Birkeland current sheet density of 1.0 μA/m.

Characteristics of Large-Scale Birkeland Currents > 50 km (0.5°)

- Stable patterns in auroral zone, cusp, polar cap (Region 1 and 2, cusp, and NBZ systems)
- Close association with large-scale convection and electric field patterns
- Close relationship to IMF
- Directly coupled to large-scale ionospheric currents detected on surface
- Carried by precipitating low-energy electrons (≤ few 100 eV) for upward flowing currents.
- Generated by solar wind/magnetospheric processes

Characteristics of Small-Scale Birkeland Currents < 50 km (0.5°

- Irregular patterns embedded in large-scale Region 1, Region 2, cusp and NBZ systems
- Close association with visible and UV auroral forms
- Close association with AKR, micropulsations, and ionospheric instabilities
- Associated with plasma processes within the magnetosphere and ionospheric processes
- Carried by high energy (10's of keV) electrons or ions

Antarctic research: main tasks for studies in relation with observations in Arctic.

The geographical conditions in Antarctica is strictly different from what we have in Arctic. The set of slides give you imagination about practical settlements for work in Antarctica.

The geophysical conditions in Antarctica is very likely to that what we have in Arctic. The main cause for that is the permanent magnetic field of Earth. The symmetry of magnet inside the Earth led to the magnetic conjudacy between Arctic and Ahtarctic. On Fig. 17 shown the conjugate map for both hemispheres. Pay attention that position of geographical and geomagnetic poles are different in both hemispheres. The system of coord nates for description of upper atmosphere phenomena is "corrected geomagnetic coordinates". Now we use the algorythm proposed by G. Gustafsson and N.Tsyganenko. The geophysical obesrvations network in Antarctica presented on Fig.18 Many stations located inside the auroral zone and special experiment was carry out in the vicinity of corrected geomagnetic pole with sovient unmanned network. The main goals of such experiments was to study the character of variations in view of results from Arctic observations. On Fig.19 the equivalent current vector over southern polar cap related with IMF are presented. Some distinct features are observed, which was not evdent from Arctic data: few gaps in structure of currents, more narrow positions of vortexes, etc.

Traditionally, many studies are devoted to conjugacy of upper atmosphere phenomena. First of all in early works E.Wescott has shown ideal conjugacy for geomagnetic variations.During differen seasons (summer-winter) it was shown the changeable conjugacy under different geophysical conditions. The conjugacy was search in auroras, particle precipitations, ionospheric parameters, etc. The conjugacy in near pole region is under the question of IMF influence. By the way the "Svaalgard-Mansurov effect", i.e. the influence of IMF on the geomagnetic variations in the near pole region was found as an output of conjugacy studies on the Vostok - Resolute Bay data.

Very interesting results was obtained at VLF transmitter at Siple by Prof. R.Helliwell from Stanford University. The experimental task was to study the VLF propagation mades and stimulation effects on particles in the magnetosphere.

The radiophysics and ionospheric sounders experiments give rise a new knowledge about processes in the southern upper atmosphere. One of the latest results concern the dynamics of polar trough according the Halley Bay station data. Besides the ground-based data recently balloon experiments was introduced in the practice of research in Antarctica. For 1988-1990 it is planned to rise international balloon program for research in Antarctica.

The scientific programs in Antarctica might be valuable and productive only with international cooperation. For this purpose all countries agreed to work together in the frame of SCAR. Upper atmosphere working group in SCAR agreed that three specialist working parties should be established during 1986-1990 for three topical interest :

1. on the depletion of ozone over Antarctica
2. using new methods of sounding the ionosphere
3. using automatic geophysical observatories.

The programs in Antarctica carried in conjunction with future international programmes:

1. The Polar Auroral Dynamics (PAD) project (1986-1989) of SCOSTEP
2. The World Ionosphere/Thermosphere Study (WITS), 1987-1992 of SCOSTEP
3. The Solar-Terrestrial Energy Program (STEP), 1986-1995, of SCOSTEP
4. The International Geosphere-Biosphere Program (IGBP) of ICSU.

The summary of geomagnetic disturbances studies: key parameters practical results and future procpectives.

From previous lectures it becomes evident the importance of geomagnetic disturbance studies. The geomagnetic field serves as a reference level for every search in magnetosphere physics. In this view most widely used data is AE and DST geomagnetic indixe That indexes have clear physical sense and shows main features of magnetospheric disturbances under ifluence of solar wind parameters. But still we have many unsolved questions concernin the magnetospheric substorm itself. With improvments the experimental technique the new results and the new knowledge led us to more understanding of physical processes.

In recent works they pay great attention on the behaviour of boundary layers, first of all on the processes on the magnetopaus On Fig.21 one can see the model for interrelations between the dayside magnetopause processes and aurora obserations in the oval according C.-I.Meng. From this pattern evident the importanc of magnetopause as a source of disturbances. The large-scale processes in the magnetosphere develops under IMF control. On Fig.22 it shown the IMF parameters and AE-index for CDAW-6 event study. But small-scale features of the interaction are also important. On the Fig.23 the flux-transfer event pattern is demonstrated. Such elemetary action led to the energy transfer from solar wind to the magnetosphere. In physical sense it lead to the very unstable behaviour of the magnetopause and ever boundary layer in the magnetosphere. On Fig.24 one can see the instability pattern on the magnetopause boundary layer and plasma sheet. From analysis of ground-based geomagnetic data it was inferred that polar geomagnetic disturbances consist from two main parts DP1 and DP2. The corresponding large-scale current loops in the magnetosphere are presented on Fig.25 and Fig.26. According recent studies this two basic parts interpreted as manifestation of "driven" and "unloading" processes. On Fig.27 shown the substorm as a mixture of this processes according D.Baker. The energy input from the solar wind to the magnetosphe goes into convective dissipation in the ionosphere and this has been termed the "driven" aspect of substorm dissipation. A major part of the solar wind energy input also goes into the form of stored energy in the Earth's magnetotail. To be a substorm there has to be at least one episode of explosive dissipation. This explosive dissipation phase represents the "unloading" of energy that was previously stored in the magnetotail. Some of the unloaded energy eventually appears in the inner magnetosphe ionosphere in the form of ring current enhancement, ionosphere Joule heating, and auroral particle precipitation, while the re of it is returned to the solar wind, probably in the form of a severed portion of the magnetotail i.e. the "plasmoid". Let us summarise the modern concept for magnetospheric substorm. Fig.27 presents a noon-midnight meridional cross-section of the magnetosphere. The incoming solar wind plasma is collisionless its flow speed in the range of 300 to 800 km/s. Since upstream sound speeds are typically 50 km/s and Alfvén speeds are typica 100 km/s, the solar wind flow is highly supersonic and superalfvenic, Alfven Mach numbers M_A=3÷10. A southward turning of the IMF initiates enhanced solar wind reconnection with terrestrial field. Dayside magnetospheric flux is eroded, and field lines a dragged across the polar caps into the nightside tail lobes. As flux is continually, and rapidly, added to the lobes, the plasm sheet gradually thins. A plasma sheet instability eventually occurs, which causes a new neutral line to form in the near-Earth tail region. There is then greatly enhanced reconnection plasma sheet and, eventually, lobe field lines which rapidly dissipates stored magnetic energy. When reconnection has proceeded sufficiently, a large segment of the plasma sheet is severed and lost in the form of a plasmoid which then rapidly carries away great amounts of the stored energy in the tail. Th plasma sheet instability that gives rise to the new substorm-associated neutral line is probably an ion tearing mode instabi lity. The magnetospheric substorm studies are very important in vie of energy dissipation in the magnetosphere. These energy budget and time scales shows what are the dominant processes in the magnetosphere. The brief review of energy balance in the system "solar wind-magnetosphere" is presented in Appendix 3. On Fig.28 is shown a comparision of solar wind energy input to the magnetosphe compared to a measure of magnetospheric substorm energy output for CDAW-6 evnt.

In this lecture we briefly put overview on the main sources of magnetospheric substorm and processes of energy dissipation in the "solar wind-magnetosphere" system. As futur prospectives are the studies of physical mechanisms and quantative models of magnetospheric substorms which give us the possibility for their practicle use.

Energy of the magnetosphere

In the visible light, the Earth intercepts appoximately $W_s = 1.74 \cdot 10^{24}$ ergs/sec. For solar wind, the bulk flow of several hundred km/sec. corresponds to ~ 1 KeV per solar wind ion. For range apeed 300-800 km/sec and densities 1-10C cm^{-3}, the kinetic energy flux range of $W_k \sim 0.05$ -:20 ergs/cm^2·sec if the earth magnetosphere have radius $\sim 20\ R_E$, the total power intercepted due to the solar wind kinetic energy is

$W_k \sim 5 \cdot 10^{19} - 10^{22}$ ergs/sec.

The IMF energy density $B^2/8\pi$ ranges from about 10^{-10} to $4 \cdot 10^{-}$ ergs/cm^3. Taking into account the possible range of solar wind convective speeds, the magnetic energy flux is in the appoximat range $W_B \sim 0.003$-0.3 ergs/cm^2·sec Again using a magnetospheri collection cross-section of radius $20\ R_E$ gives a total intercep ted magnetic power of $W_B \sim 10^{18} - 10^{20}$ ergs/sec. This valu is appoximately 1% of the kinetic energy power of the solar wind and is of order 10^{-5} of the solar radiant energy rate striking the Earth. This value is approximately 1% of the kinetic energy power of the solar wind and is of order 10^{-5} of the solar radiant energy rate striking the Earth.

Much effort has gone into empirical determinations of how the solar wind magnetic energy couples into the magnetcspheric system. The geoeffective magnetic energy, i.e., the solar wind input energy is given by a product of the form

$$W_{in} = k_o\ V \cdot \frac{B^2}{8\pi} F(\Theta)$$

In this equation, V is the solar wind speed, B is the IMF strength, k_o is a geomagnetic parameter, and $F(\Theta)$ is a factor which accounts for the strong dependence of the energy coupling upon the polar angle Θ between the IMF and the Earth's dipole axis. For $0 \leq \Theta \leq \frac{\pi}{2}$, very little energy coupling (i.e., dayside reconnection) occu s. For $\Theta \sim \pi$ the coupling (dayside reconnection) is very efficient. Roughly speaking, a maximum energy coupling occurs when for the case of $F(\Theta) = 1$ and $k_o = \pi r^2 = \pi (20\ R_E)^2$. A more refined analysis shows that a better approximation may be

$$F(\Theta) = \sin^4 \left(\frac{\Theta}{2}\right)$$

with the definition

$$\frac{k_o}{\pi} \sim \ell_o^2$$

and $\ell_o \sim 7\ R_E$. Thus, a popular energy coupling relation in current use is

$$W_{in} \sim \ell_o^2 \cdot V \cdot B^2 \cdot \sin^4 \left(\frac{\Theta}{2}\right)$$

The substorm model predicts a repeatable sequence of events in term of solar wind energy input and storage and energy release from the magnetotail.

The rate and form of energy input to the magnetosphere is fairly well-established and the substrom may be viewed as the fundamental energy realease element permitting the return of th magnetosphere to its ground state. Examination of W_{out} traditionally concentrated upon three primary forms of substorm energy dissipation

(1) Auroral particle precipitation;
(2) Auroral Joule heating; and
(3) Ring current flows.

During substorms there are large auroral displays which are caused by energized electrons bombarding the upper atmosphere From the brightness and area of such displays, one can estimate the precipitation energy dissipation involved. Glooally--integrated energies for this dissipative component are of the order of 0.5 - 1.0 X 10^{18} ergs/sec during most substorms.

Substorms also have magnetic effects are due to strong field-aligned (Birkeland) currents that flow in the auroral zon which close (and dissipate energy resistively) in the upper ionosphere. This Joule heating associated with substorm current can also be monitored from Earth through arrays of magnetomete and ionospheric conductivity models can be employed to convert measured currents to ohmic (I^2R) dissipation. Global numbers fc this component of dissipation are typically 1-5 10^{18} ergs/sec during most substorms.

Trapped particles drifting in the Earth's inner magnetospheric region constitute ring current. A large enhancement of this ring current can cause large magnetic disturbances in the equatorial magnetic field at Earth's surface. During many storm intervals, accelerated particles and hot plasma are injected from the tail into the ring current. There the energy of these particles is gradually (over hours or days) lost due to precipitation and charge exchange processes.

During even quiet times, the ring current contains an energy comparable to that stored in the magnetotail: $\sim 10^{22}$ ergs. During a typical substorm, the ring current energy can grow at a rate of 2-3 x 10^{18} ergs/sec, while during intense storms it may grow by as much as 10^{19} ergs/sec.
Therefore, a significant part of the energy dissipation during substorms can be assessed by examination of auroral and ring current terms. The total energy dissipation W_{out},

$$W_{out} = W_{RC} + W_A + W_J$$

where W_{RC} is ring current loss, W_A is auroral precipitation, and W_J is Joule heating loss.

It has been suggested that W_A and W_J scale directly with AE (in nT):

$$W_A = 1 \times 10^{15} \text{ AE}$$

and

$$W_J = 2 \times 10^{15} \text{ AE}$$

The W_{RC} term is estimated to be related to Dst and its time derivative:

$$W_{RC} = 4 \times 10^{20} \left(\frac{\partial Dst}{\partial t} + \frac{Dst}{\tau}\right)$$

with τ being a charge-exchange lifetime (several hours).

On Fig.28 we can eximine the relationship between input and output energy processes for a particular substrom event on Marc 22, 1979.

The total energy dissipated to the Earth and to the inner magnetosphere during substorms is often less than half of the energy that was stored and released from the magnetotail. This raises the question of what becomes of the other very substantial fraction of the energy. It seems likely that it is released direct to the down-stream solar wind in the form, first, of a plasmoid and then as energized plasma flowing tailward directly from the reconnection region. Substorms represent the extraction, storage, and delayed dissipation of energy from the flowing solar wind. From a total solar wind power of order 10^{21} ergs/s, 10^{18}-10^{19} ergs/s typically enter the magnetosphere. Of this entering energy perhaps 50% is converted to geoeffective forms while the remainder is released back into the downstream solar wind.

- Kamide Y., A.D.Richmond, S.Matsushita -1981- Estimation of ionospheric electric fields, ionospheric currents and field-aligned currents from ground magnetic records. J.Geoph.Res., 86, N°A10, pp.801-
- D.N.Baker, S.-I.Akasofu, W.Baujohann, J.W.Bieber, D.H. Fairfield, E.W.Hones, Jr., B.Mauk, and R.L.McPherron, Chapter 8 - Substorms in the Magnetosphere (in Solar Terrestrial Physics - Present and Future, D.Butler and K.Papadopoulos, Eds.), NASA (1984).
- Feldstein Y.I., Zaitzev A.N. -1968- S_D-variation of the magnetic field in high latitudes with different intensity of magnetic disturbances, Annales Geoph. vol. 24, N°2 pp.1-8.
- Wescott E.M., -1966- Magnetoconjugate phenomena, Space Sci. Rew.,5, pp.507-561.
- T.A.Potemra -1985- Field-aligned (Birkeland) currents, Space Sci. Rev., 42, 295-311.
- Iijima T., Potemra T.A., -1976- The amplitude distribution of field-aligned currents at northern high latitudes observed by TRIAD. J.Geophys. Res., 81, N° , 2165-
- Iijima T., Potemra T.A. -1978- Large-scale characteristics of field-aligned currents associated with substorms. J.Geophys. Res., 83, N° , pp.599-
- Spiro R.W. Reiff P.H. Maher L.J. Precipitating electron energy flux and auroral zone conductance: an empirical model. J.Geoph. Res. 1982, vol. 87, N°10, pp.8215-8227
- G. Rostoker et. al. - 1980 - Magnetospheric substorms - definition and signatures. J. Geoph. Res. vol. 85 No. A4. pp. 1663-1668.
- Y.Kamide et. al. - 1982 - Global distribution of ionospheric and field-aligned currents during substorms as determined from six IMS meridian chains of magnetometers: initial results. J. Geoph. Res. vol. 87, No. A10., pp. 8228-8240.
- Papitashvili V.O., Zaytsev A.N., Ya. I. Feldshteyn, - 1983 - Magnetic disturbances generated by the Interplanetary Magnetic Field in the Southern Polar Cap during the summer, Geomagnetism and Aeronomy (Engl. transl.) vol. 23 No.4, pp. 506-509.
- N.S. Sastri, - 1982 - Low-latitude Bay Disturbance on 21 Mar. 1981., Ind. J. Radio Space Sci., vol. 11, pp. 213-214.
- Quantative Modelling of Magnetosphere Processes, ed. W.P. Olson, AGU, Washington D.C., 1979.
- Dynamics of the Magnetosphere, ed. by S.-I. Akasofu, D. Reidel, Hingham, Mass. 1980.

Table 1

NATURAL GEOMAGNETIC VARIATIONS

character period in sec	type of phenomena	character amplitude	geomagnetic indexes
10^{-2} … 10^{9}	VLF & ULF; P_c1; P_c2; P_c3; P_c4; P_c5; P_c6; P_i1; P_i2; SSC; bays; micropulsations; disturbances; diurnal variations; mag-storms; 27 ± day variations; annual variations; 11-year variations; secular variations; long-period variations	in nT; $\geq 0{,}01\,\gamma$; 0,1; 3 nT; 5-10; ≤ 100; ≤ 50; ~500; ≤ 50 ~500; ≤ 50; ~25nT/year	AE; D_{st}; K_p; $\sum AE$; $\sum D_{st}$; $\sum K_p$

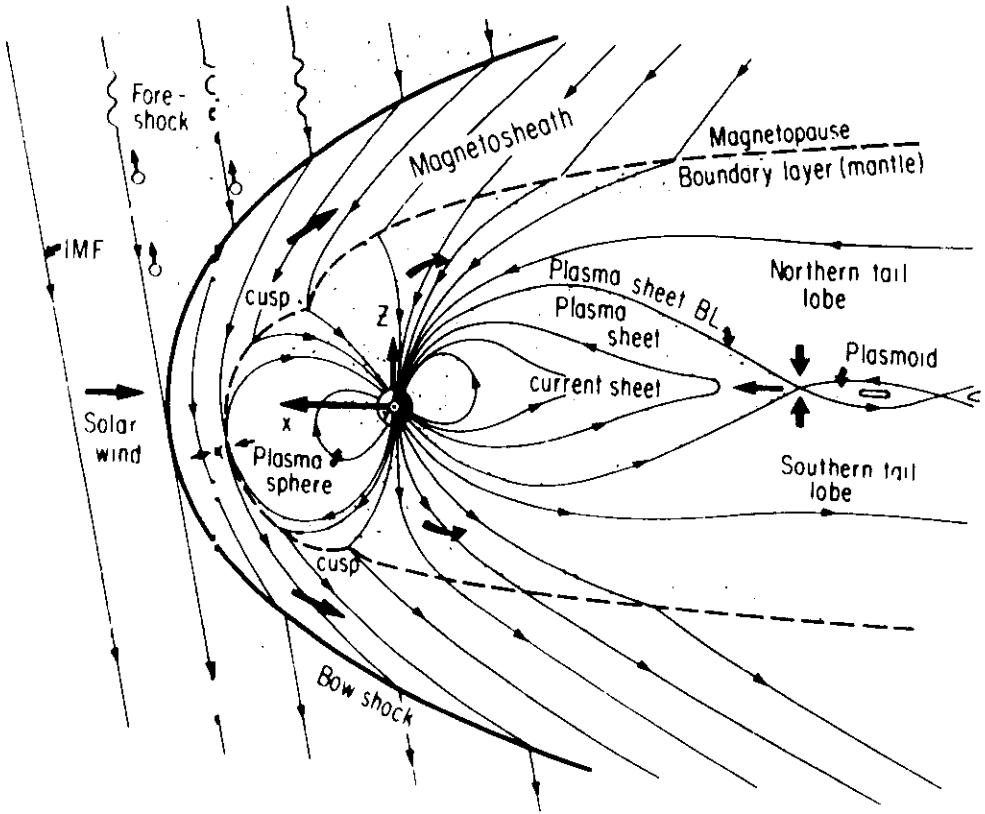

Fig. 1

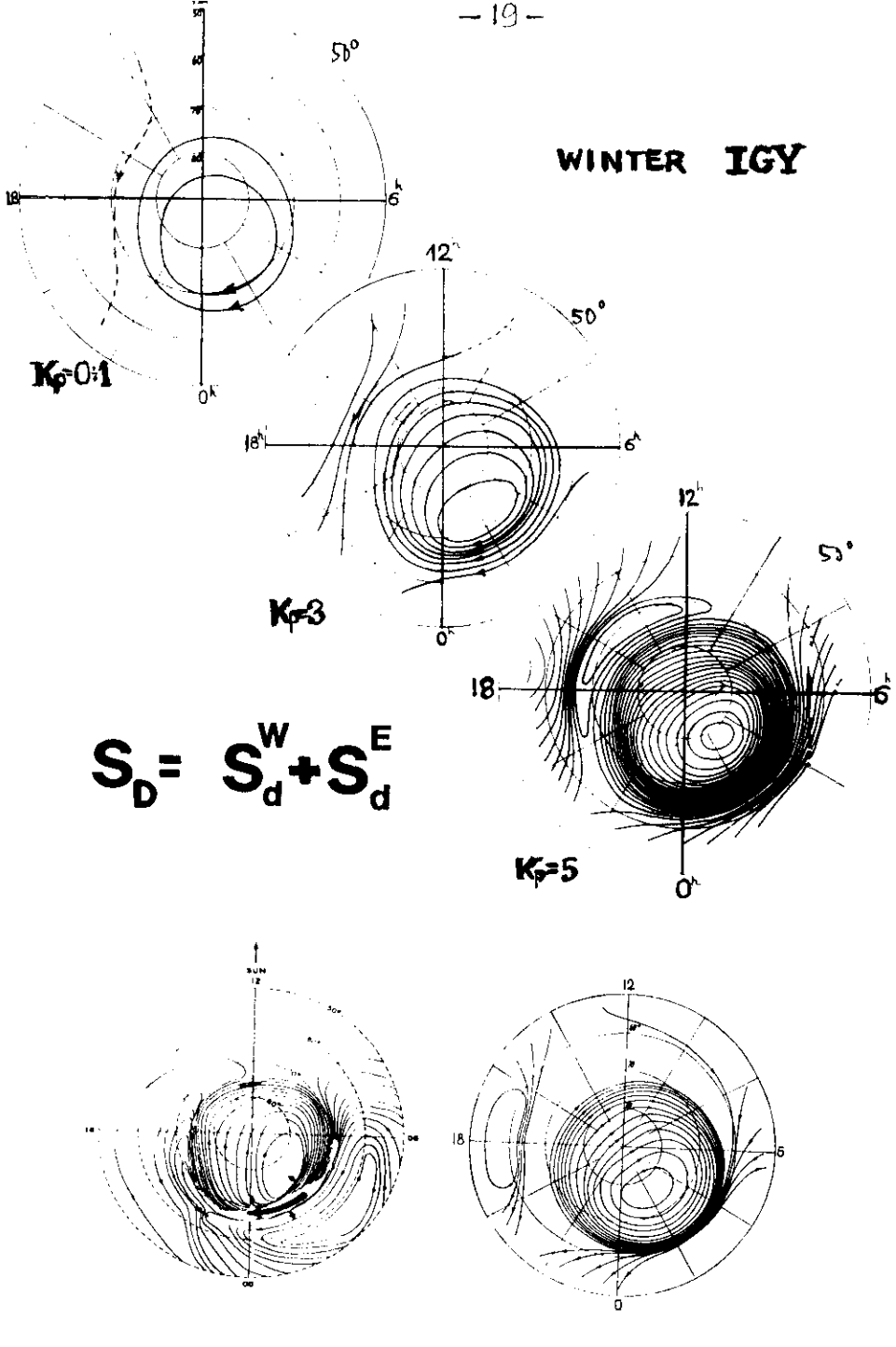
WINTER IGY
K_p=0+1
K_p=3
K_p=5
$S_D = S_d^W + S_d^E$

Fig. 2

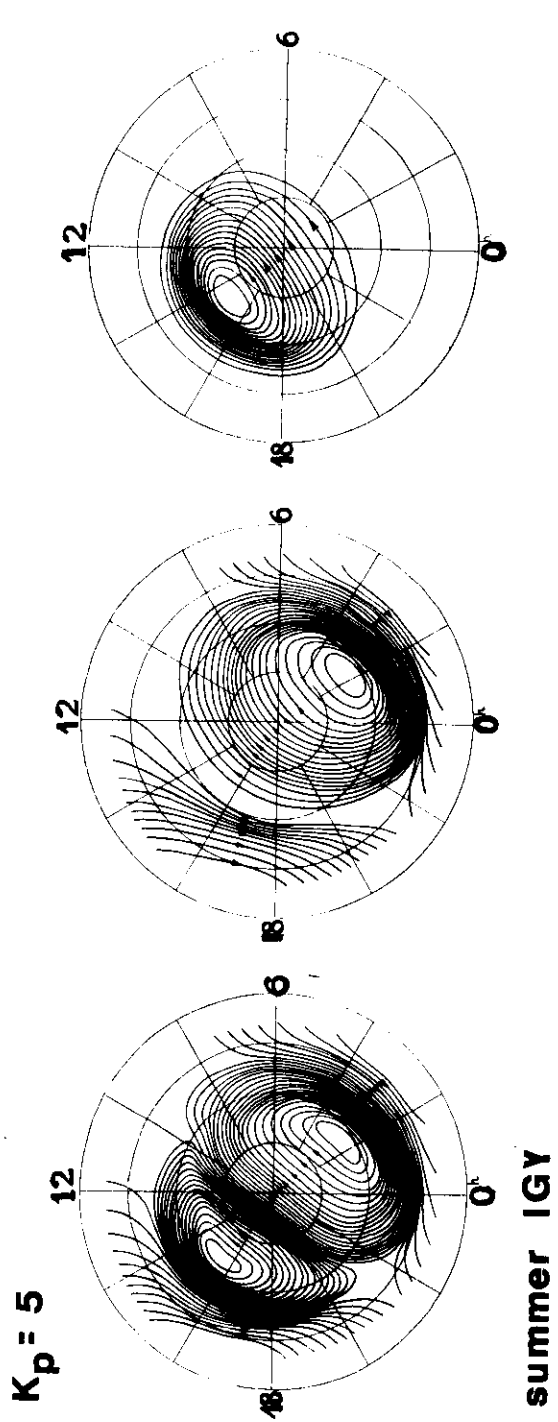
K_p = 5
summer IGY
$S_D = S_d^W + S_d^E + DPC$

Fig. 3

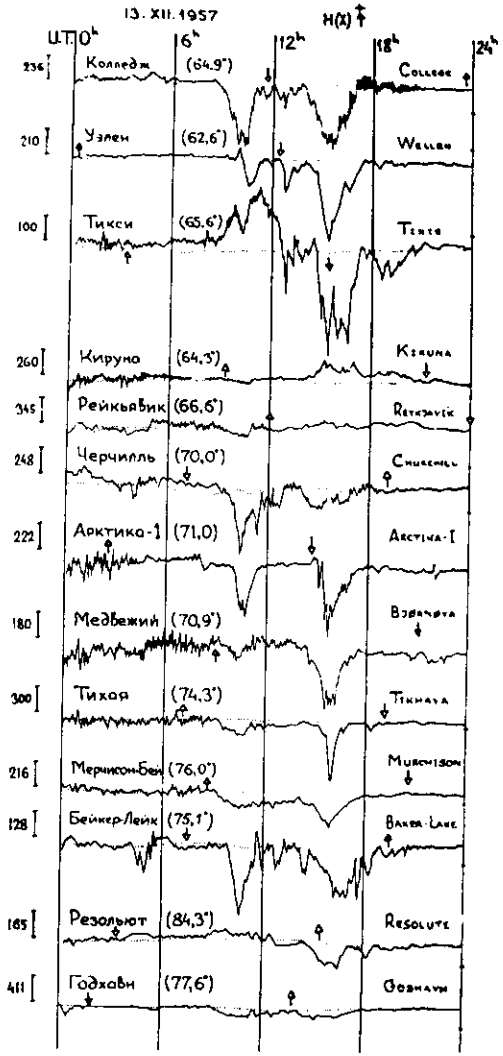

Fig. 4 $H(X)$ component of high latitude observatories in December 13, 1957. The increase of field is upward. The dotted line is the quiet field level on January 4, 1958. The midnight is indicated by the downward arrow, the noon — by the upward one for each station. In brackets the corrected geomagnetic latitude is indicated. The scale in gammes is to the left.

Fig. 4

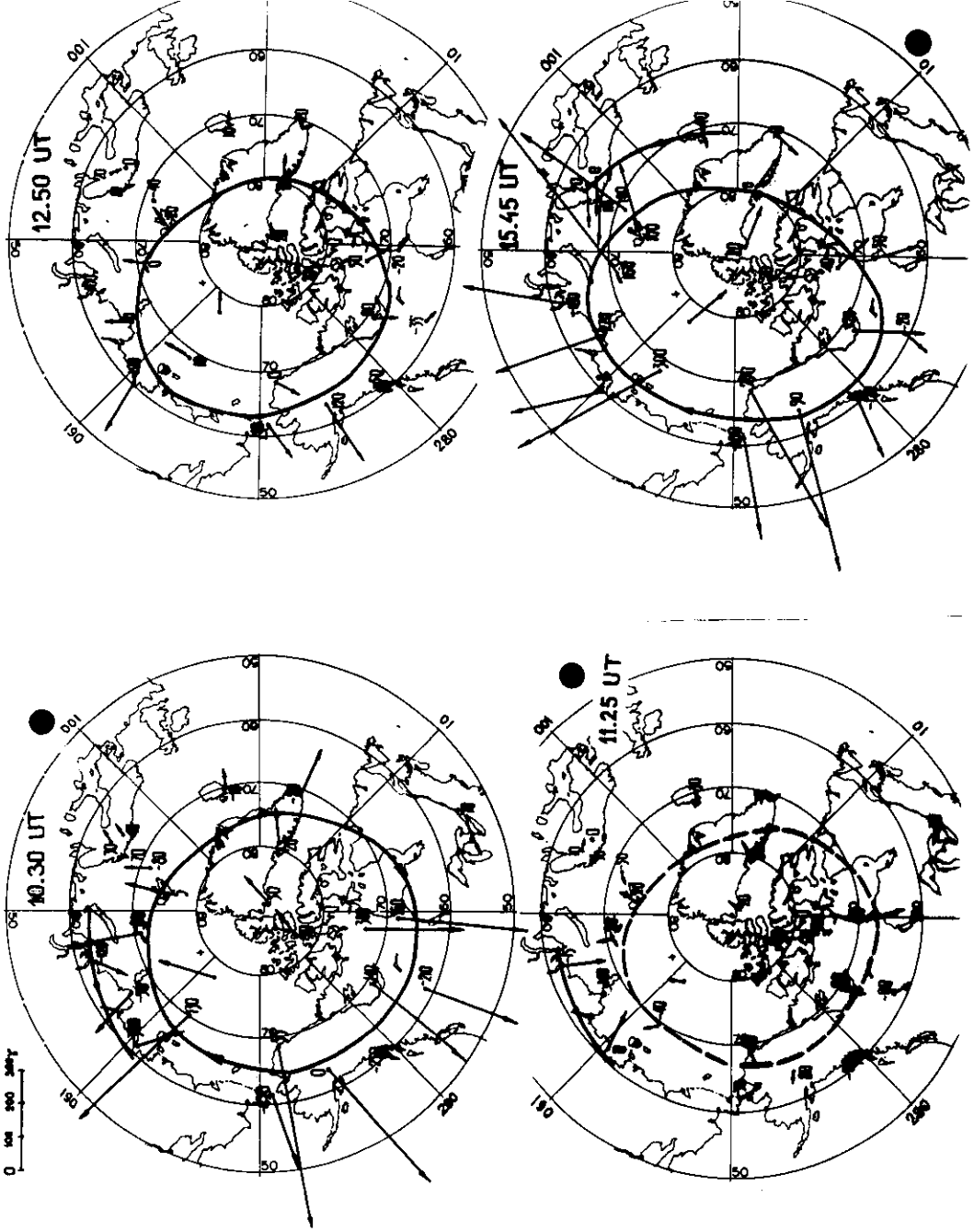

Fig. 5

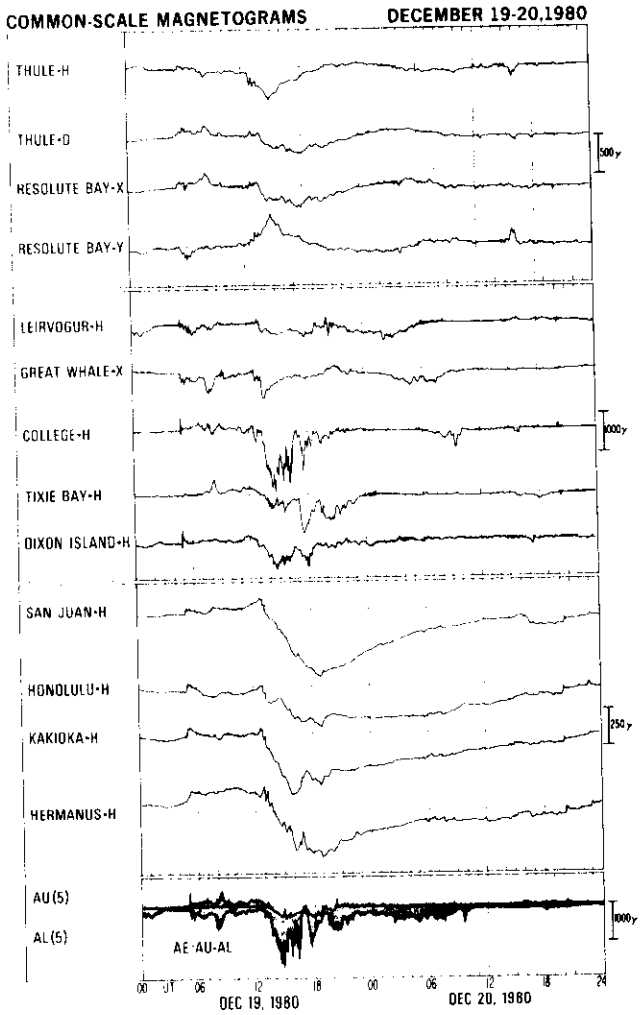
COMMON-SCALE MAGNETOGRAMS
DECEMBER 19-20,1980
THULE-H
THULE-D
RESOLUTE BAY-X
RESOLUTE BAY-Y
LEIRVOGUR-H
GREAT WHALE-X
COLLEGE-H
TIXIE BAY-H
DIXON ISLAND-H
SAN JUAN-H
HONOLULU-H
KAKIOKA-H
HERMANUS-H
AU(5)
AL(5)
AE-AU-AL
500γ
1000γ
250γ
1000γ
00 UT 06 12 18 00 06 12 18 24
DEC 19, 1980
DEC 20, 1980

Fig. 6

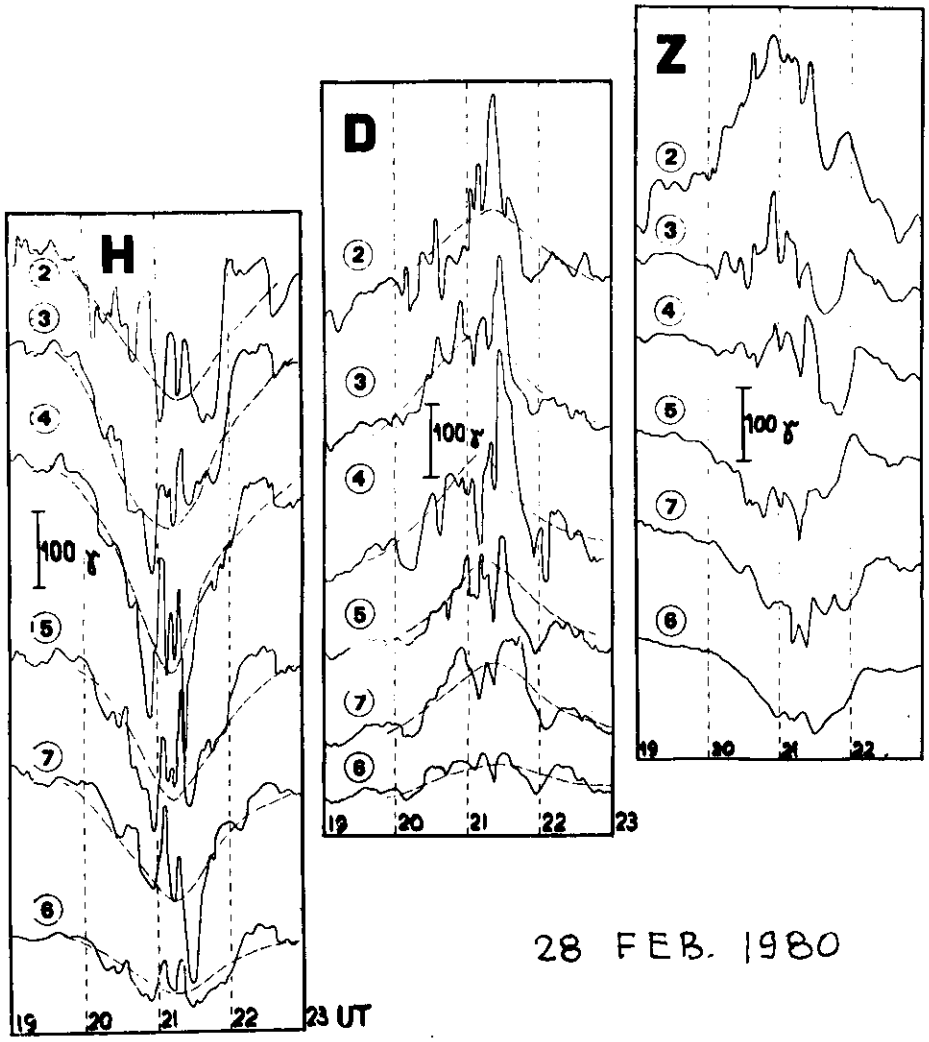
H
D
Z
100 γ
100 γ
100 γ
2
3
4
5
6
7
19 20 21 22 23 UT
28 FEB. 1980

Fig. 7-A

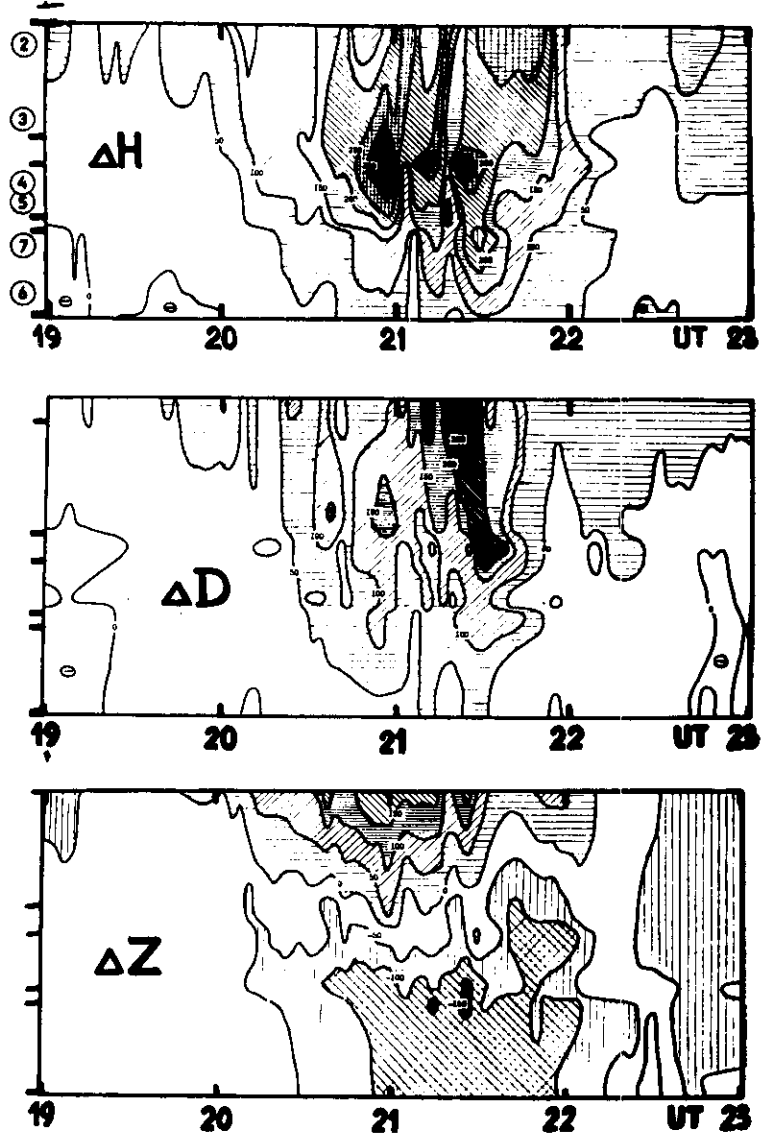

Fig. 7 - B'

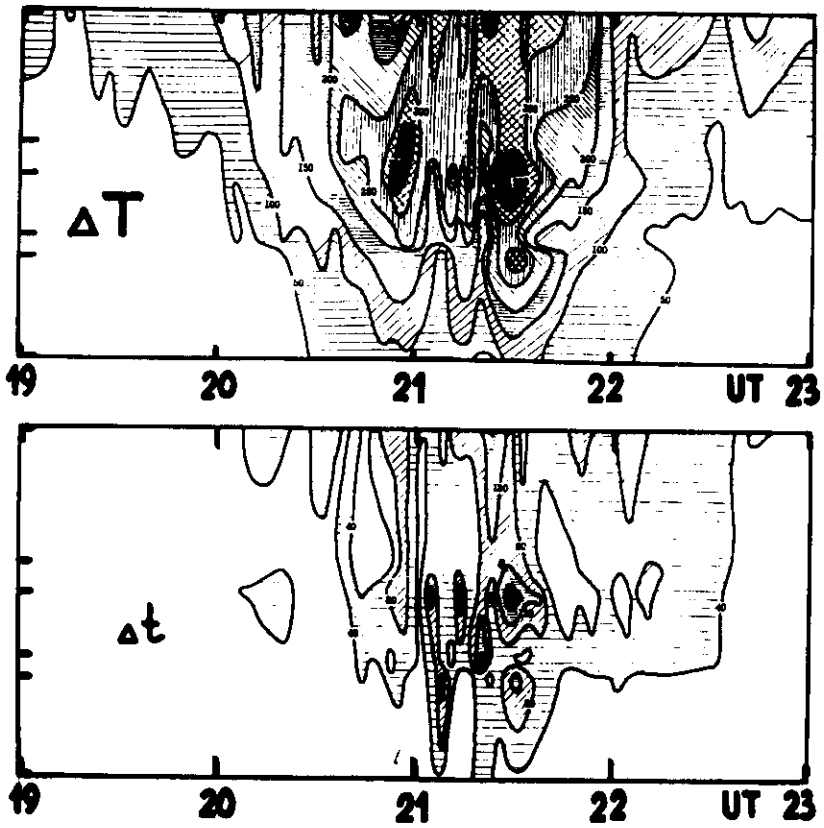

Fig. 7 - B"

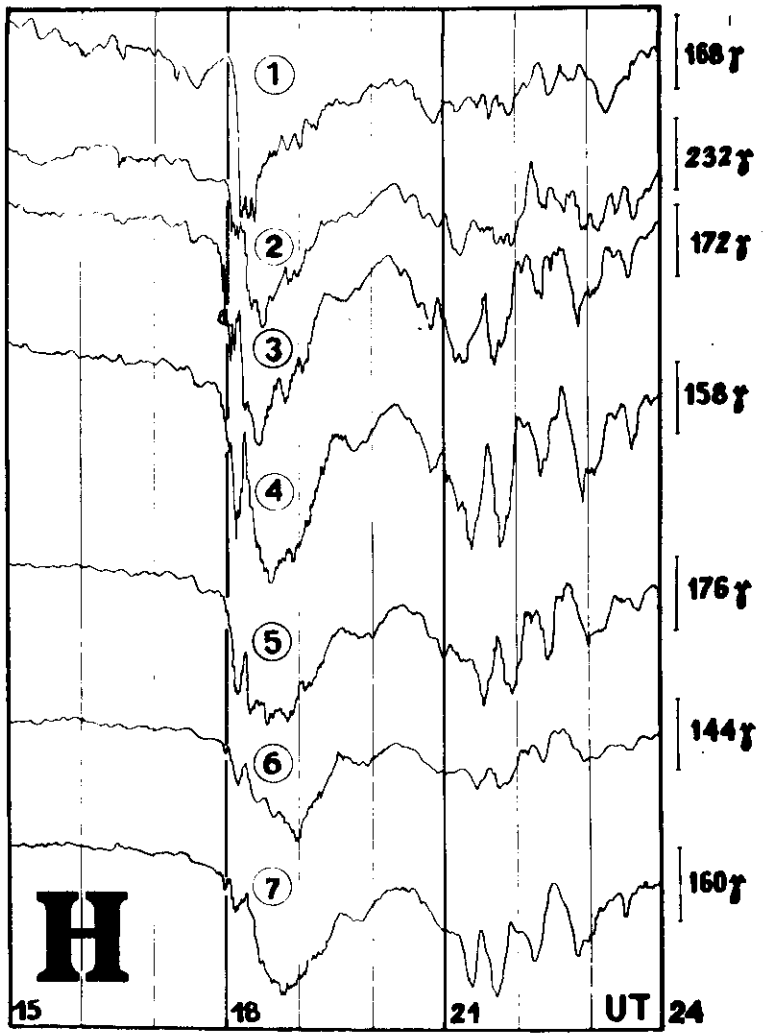
H
1
2
3
4
5
6
7
168γ
232γ
172γ
158γ
176γ
144γ
160γ
15
18
21
UT
24
28 МАЯ 1979

Fig. 8-A'

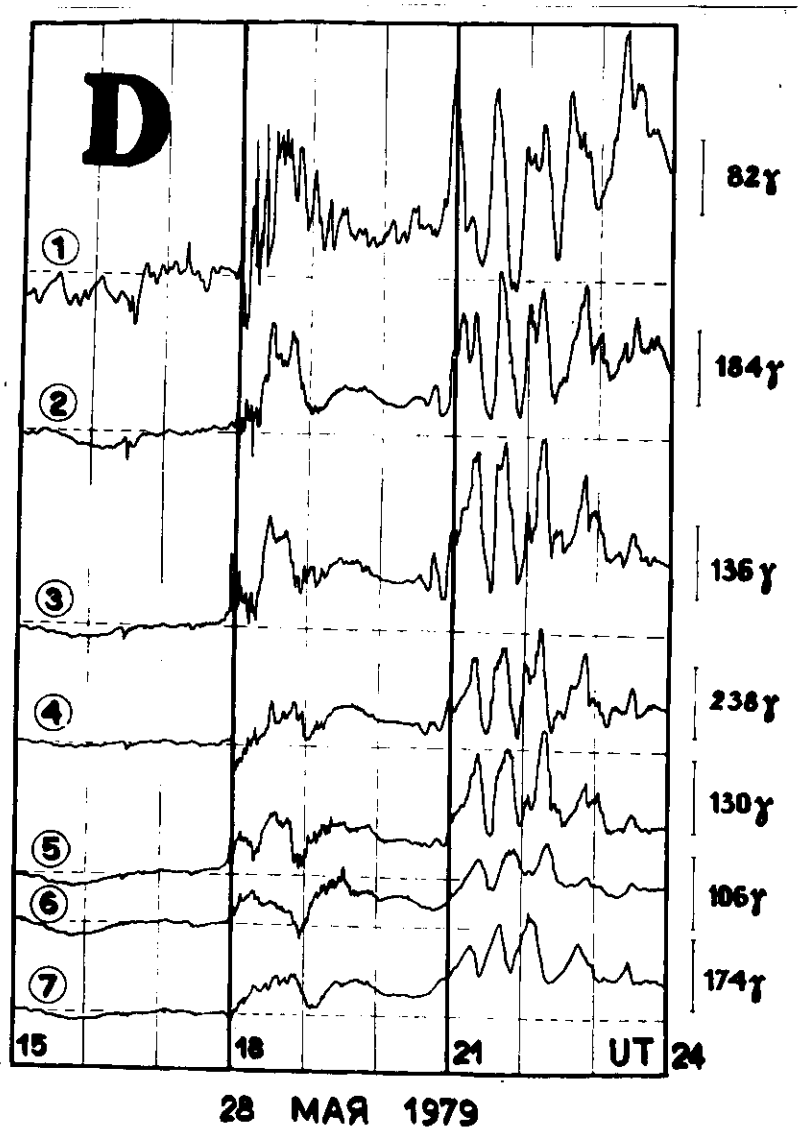
D
1
2
3
4
5
6
7
82γ
184γ
136γ
238γ
130γ
106γ
174γ
15
18
21
UT
24
28 МАЯ 1979

Fig. 8-A''

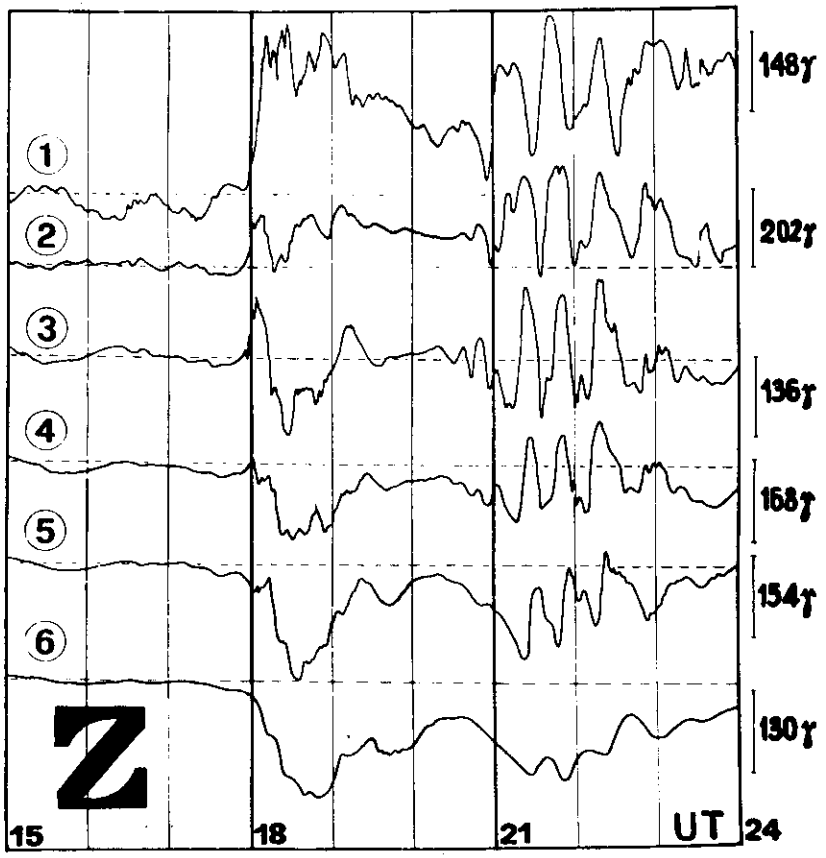

28 МАЯ 1979

Fig. 8-A'''

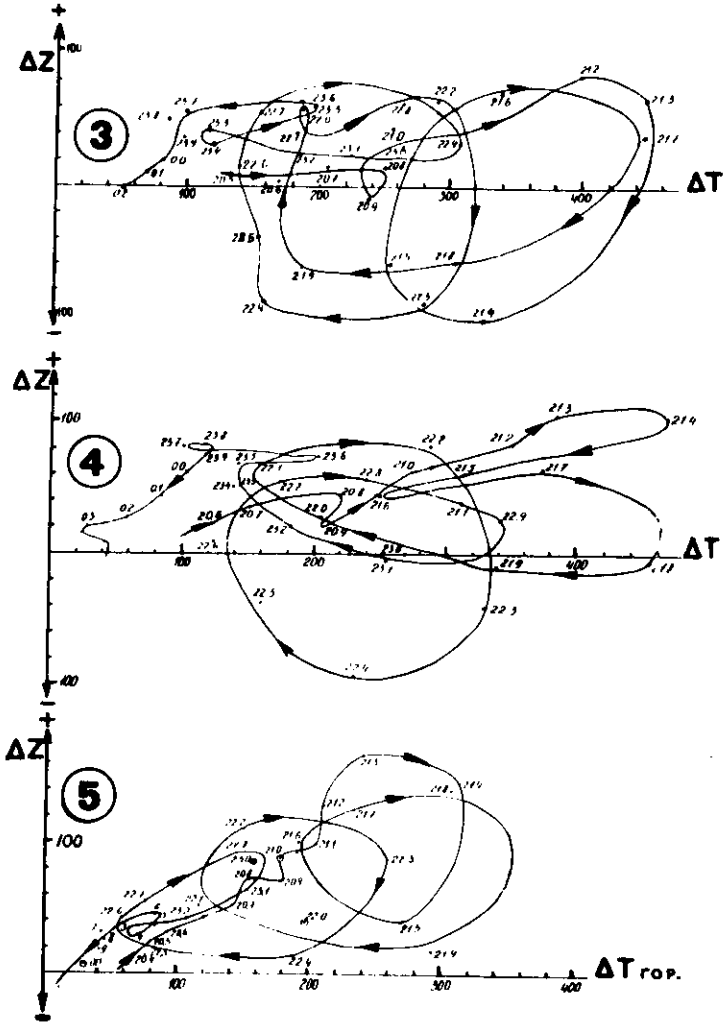

28 МАЯ 1979

Fig. 8-B

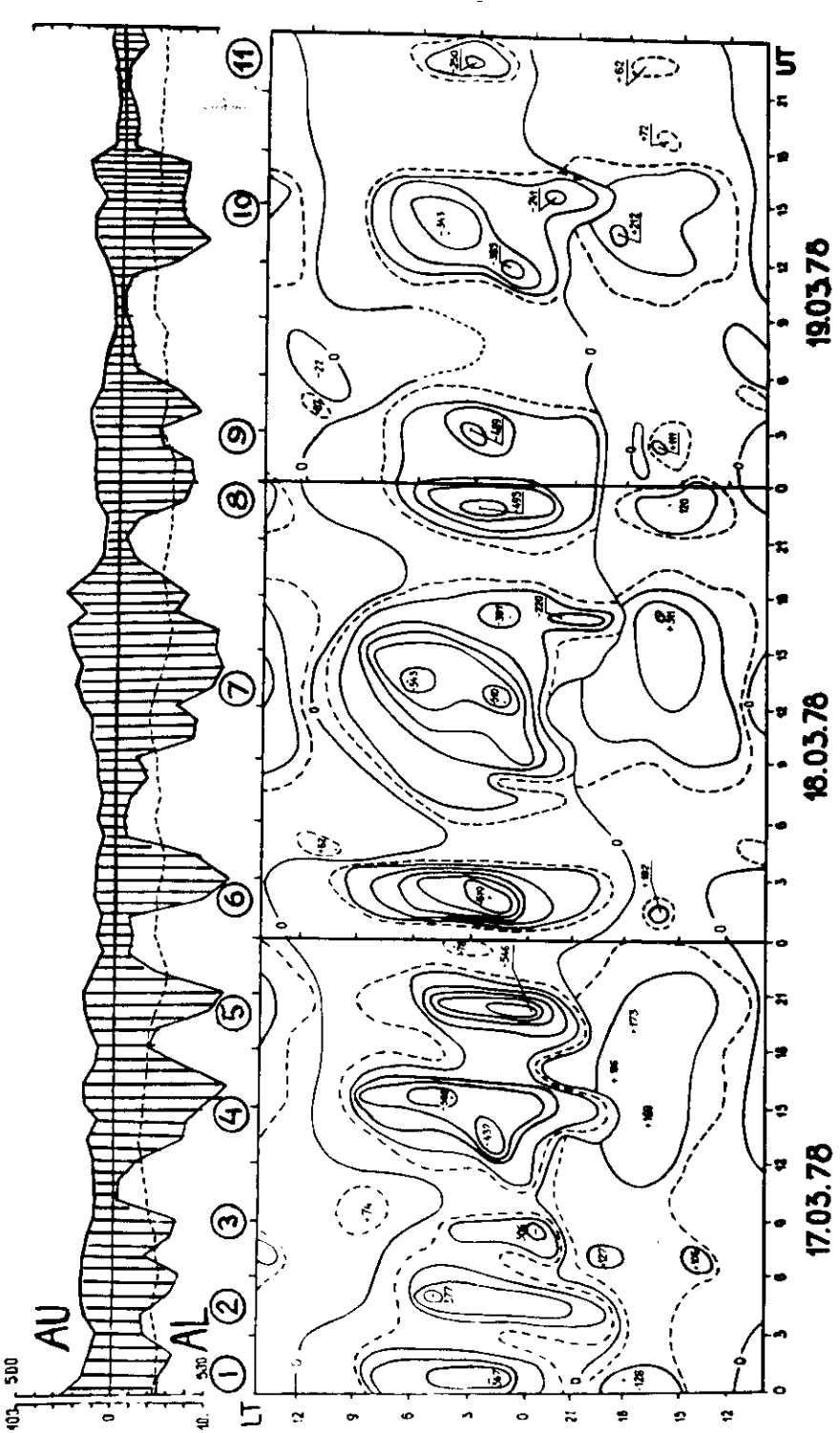

Fig. 9

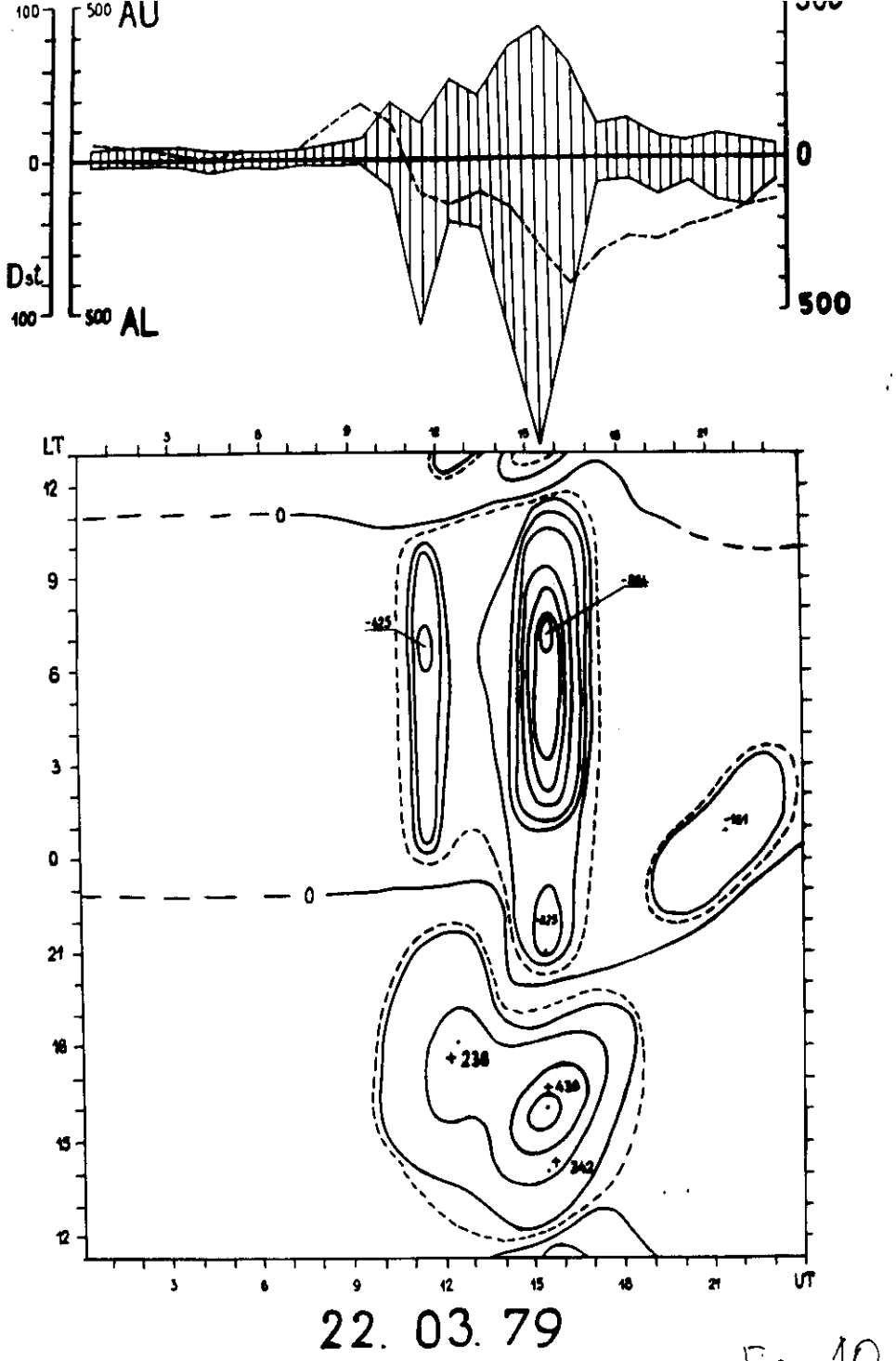

Fig. 10

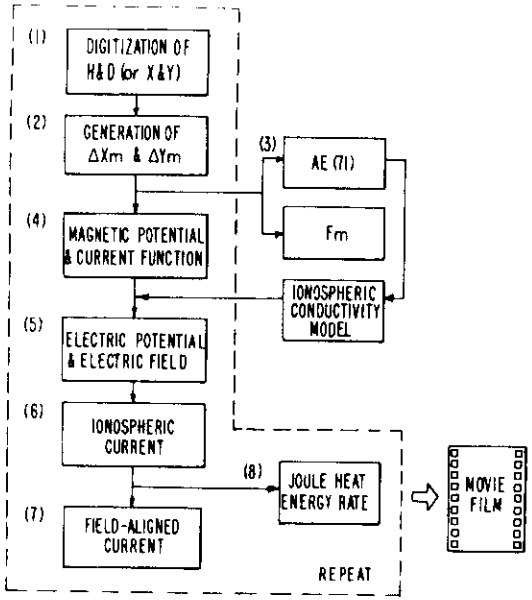

Fig. 11

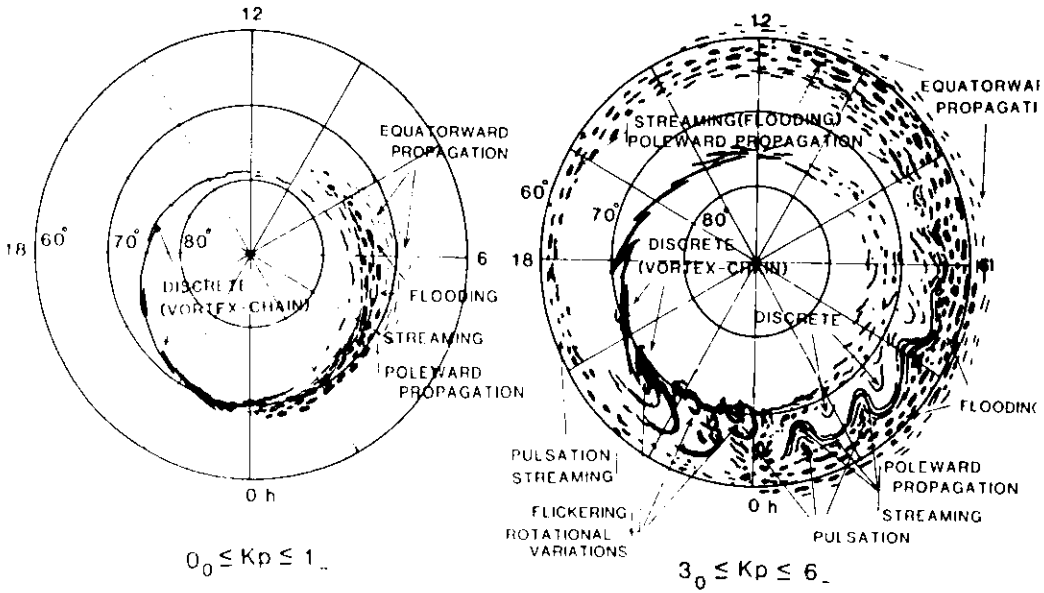

Fig. 15

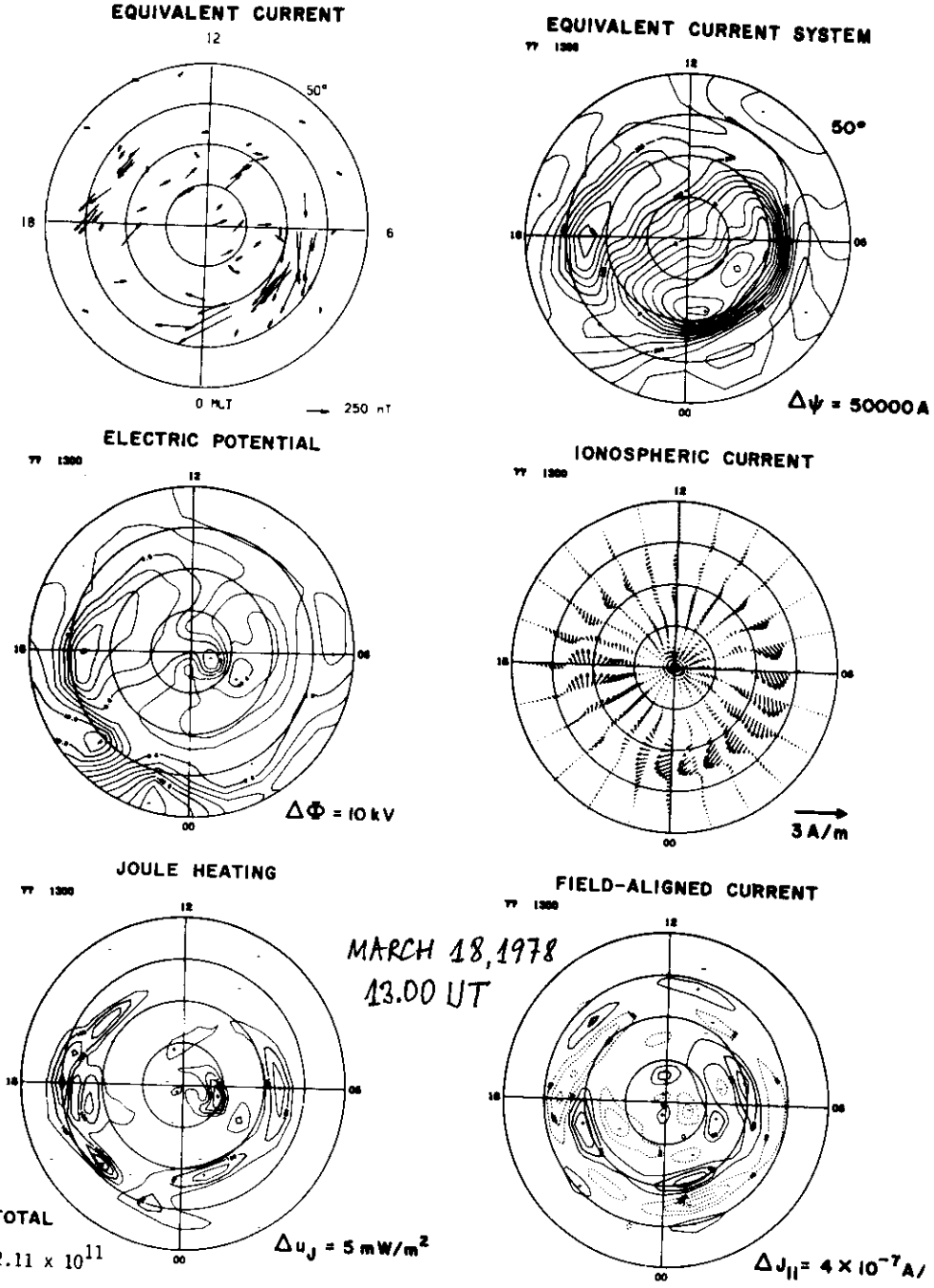

Fig. 12

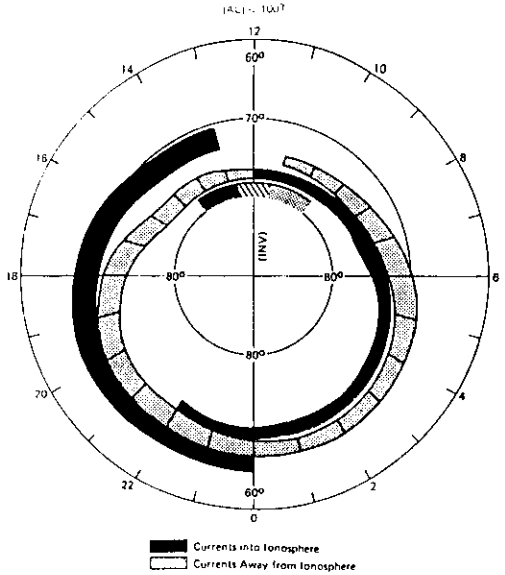

Fig. 13

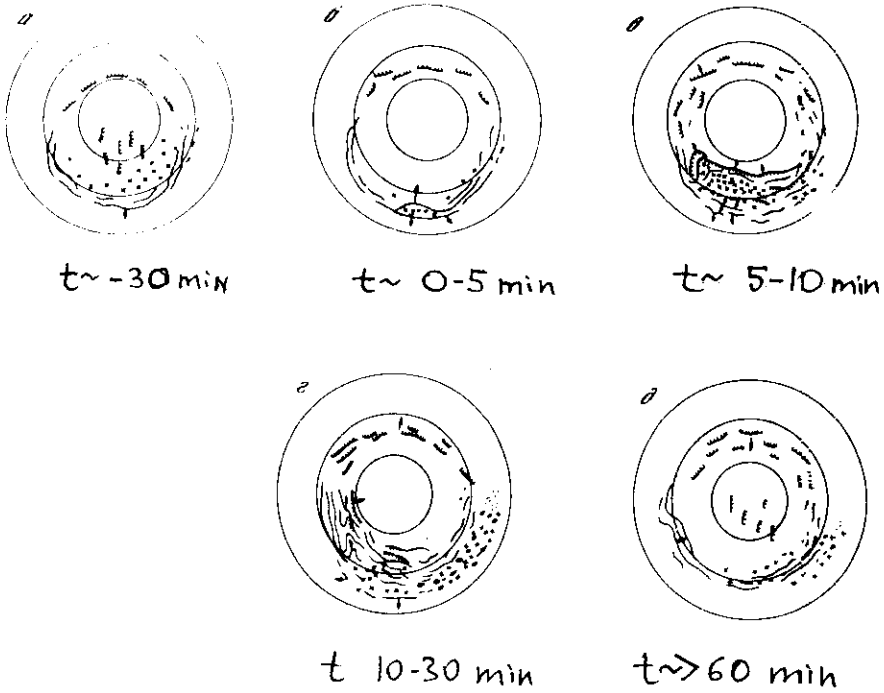

Fig. 14

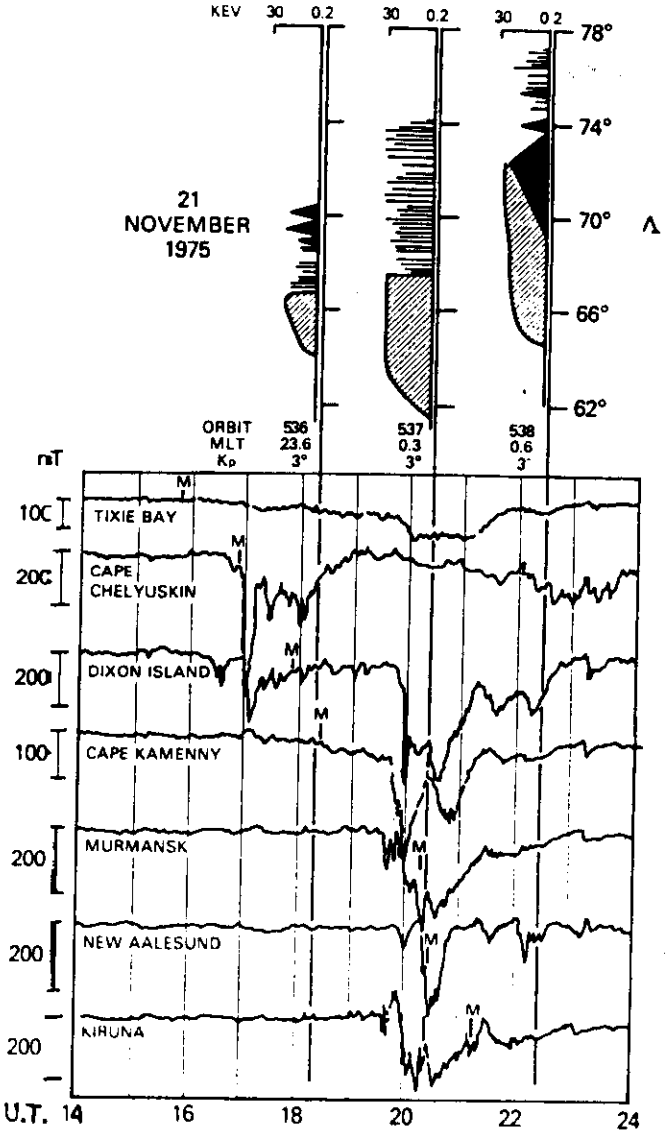

Fig. 16

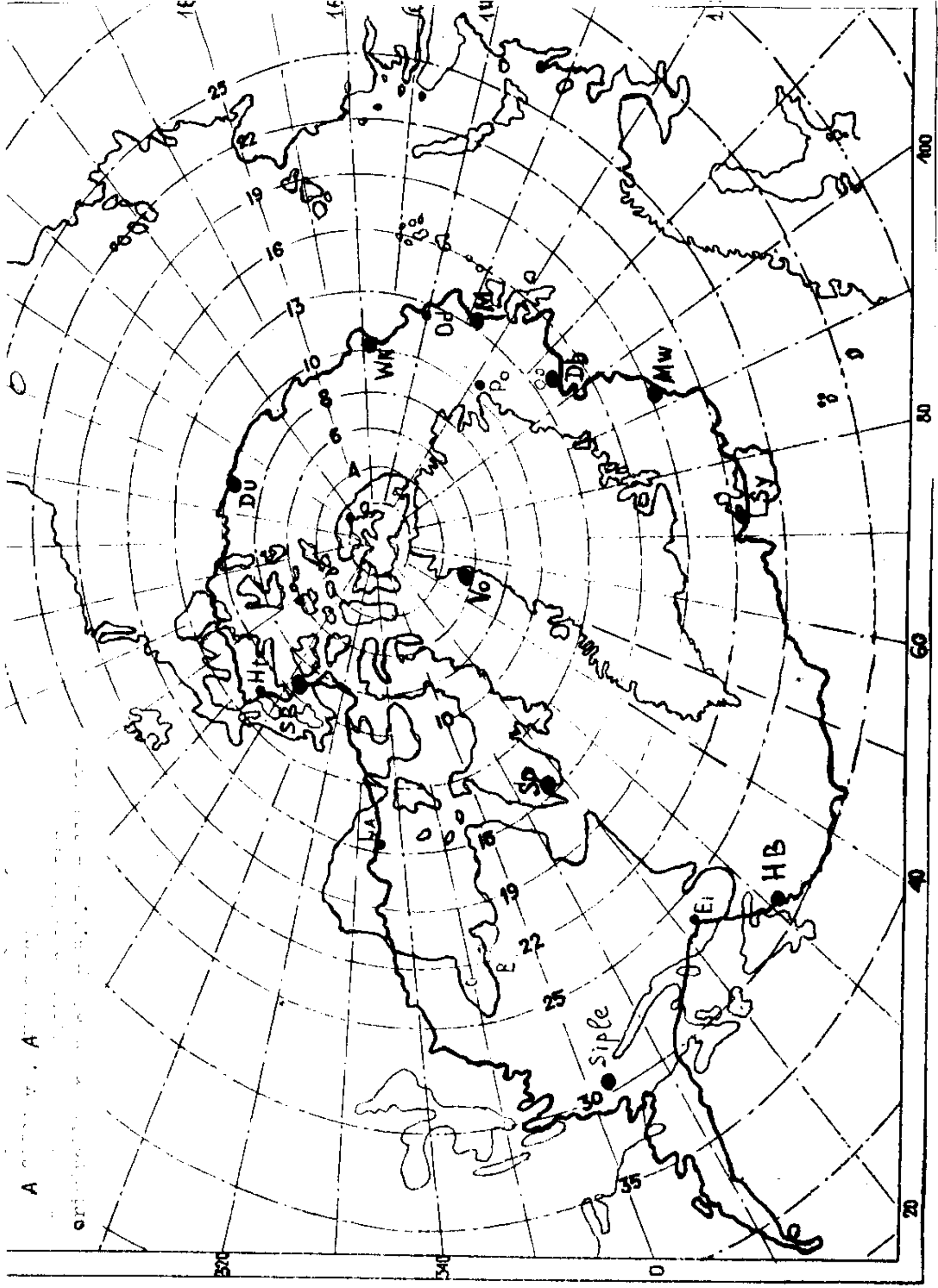
Siple
HB
Ei
DU
Wk
No
Mw
Sy

Fig. 17

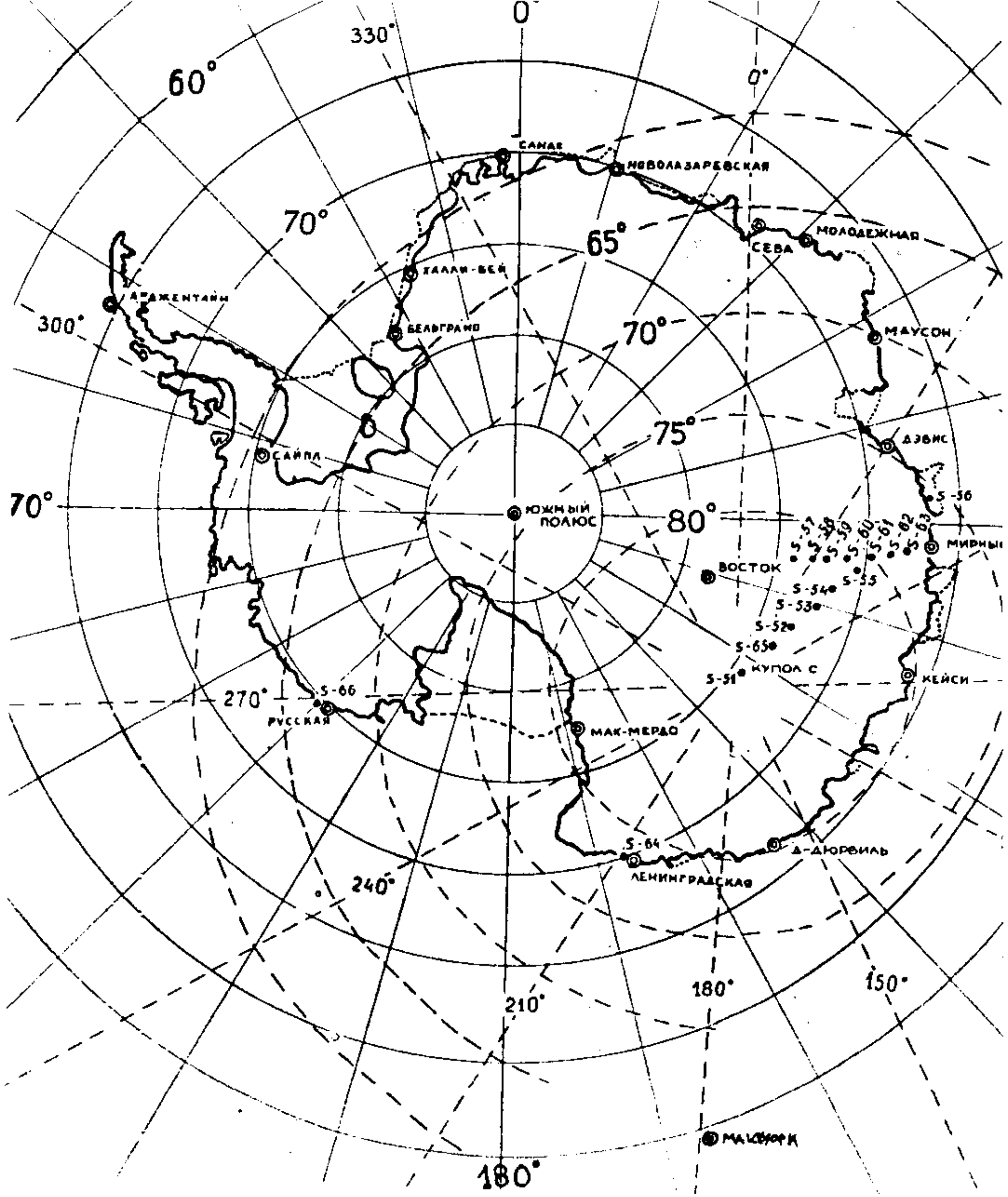
0°
330°
60°
70°
65°
75°
80°
300°
270°
240°
210°
180°
150°
САНАЕ
НОВОЛАЗАРЕВСКАЯ
МОЛОДЕЖНАЯ
СЕВА
ХАЛЛИ-БЕЙ
БЕЛЬГРАНО
МАУСОН
ДЭВИС
САЙПЛ
ЮЖНЫЙ ПОЛЮС
ВОСТОК
КУПОЛ С
КЕЙСИ
МАК-МЕРДО
РУССКАЯ
ЛЕНИНГРАДСКАЯ
Д-ДЮРВИЛЬ

Fig. 18

Soviet Unmanned Magnetometer Network in Antarctica

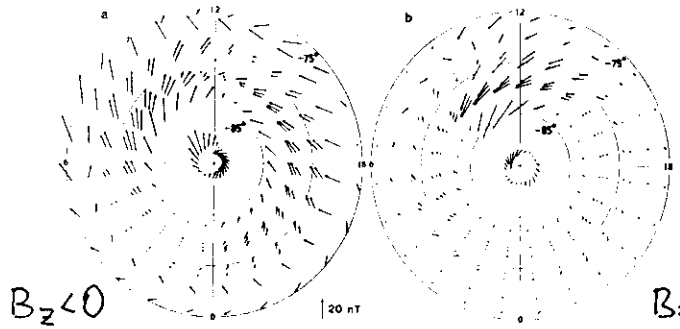

The Variation Controlled by the B_z Component of the IMF

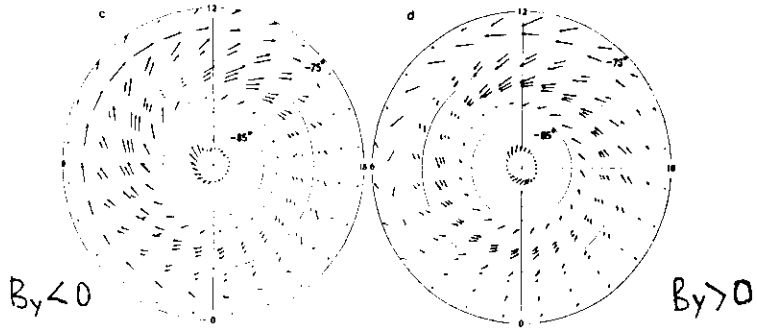

The Variation Controlled by the B_y Component of the IMF

The equivalent current vector distributions over the southern polar cap related to the IMF: a) $B_z<0$; b) $B_z>0$; c) $B_y<0$; d) $B_y>0$. Arrows indicate the scale factor 20 nT. Corrected geomagnetic latitude (Φ') —magnetic local time (MLT).

Fig. 19

Fig. 21

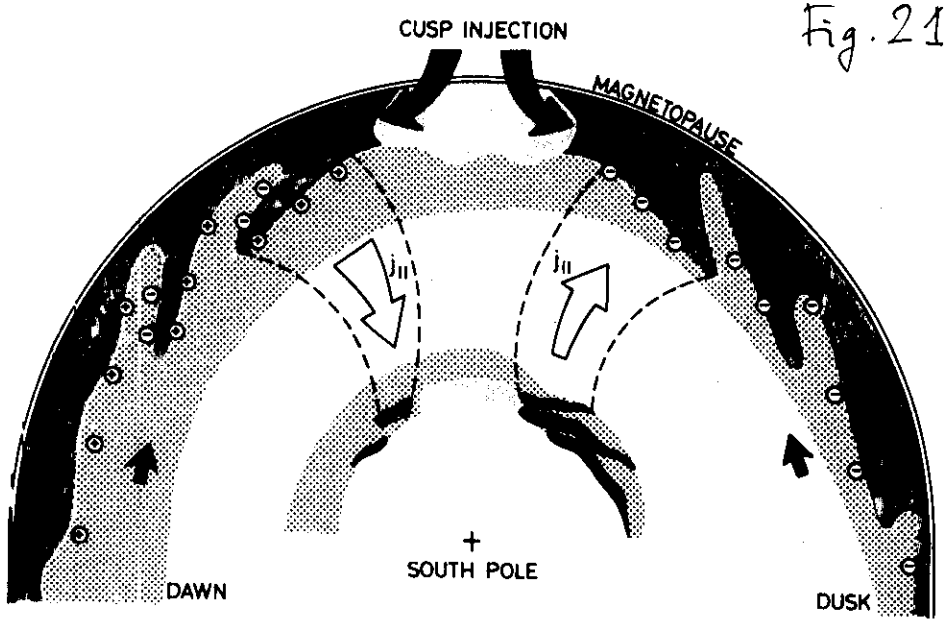

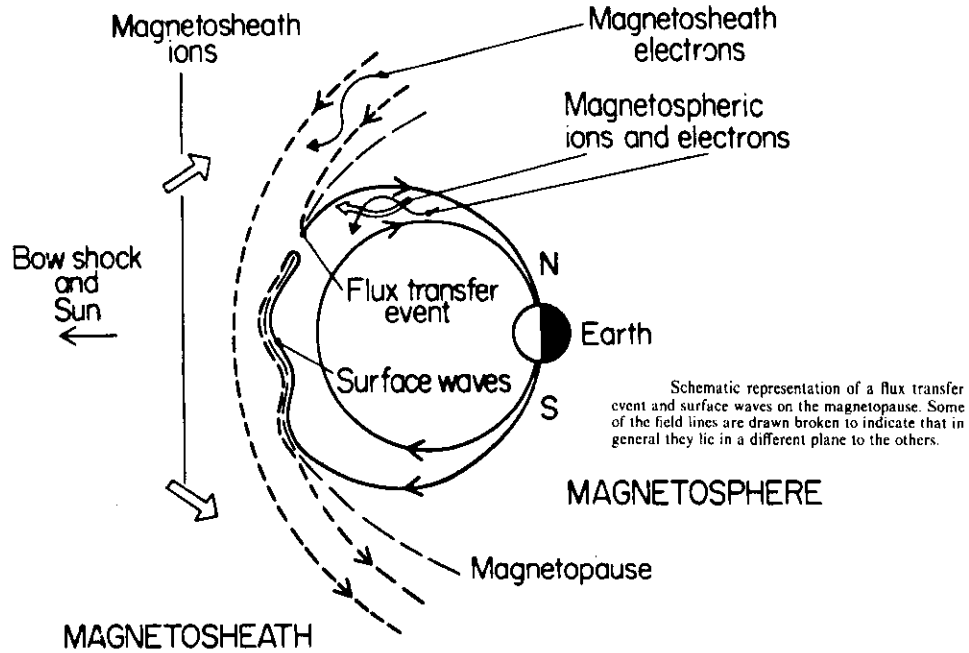

Schematic representation of a flux transfer event and surface waves on the magnetopause. Some of the field lines are drawn broken to indicate that in general they lie in a different plane to the others.

Fig. 23

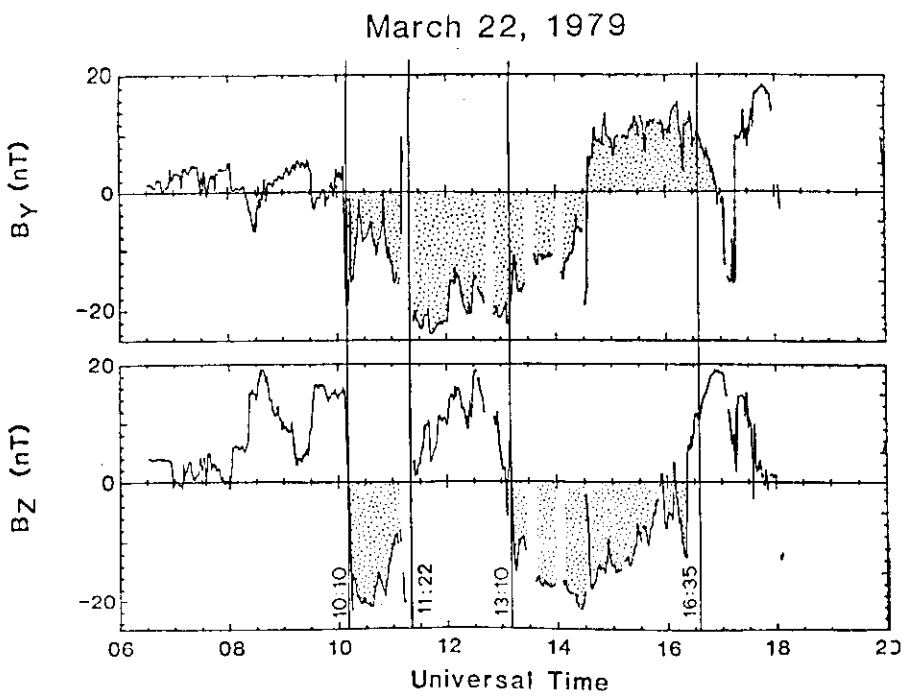
March 22, 1979
B_Y (nT)
B_Z (nT)
20
0
-20
10:10
11:22
13:10
16:35
06
08
10
12
14
16
18
20
Universal Time

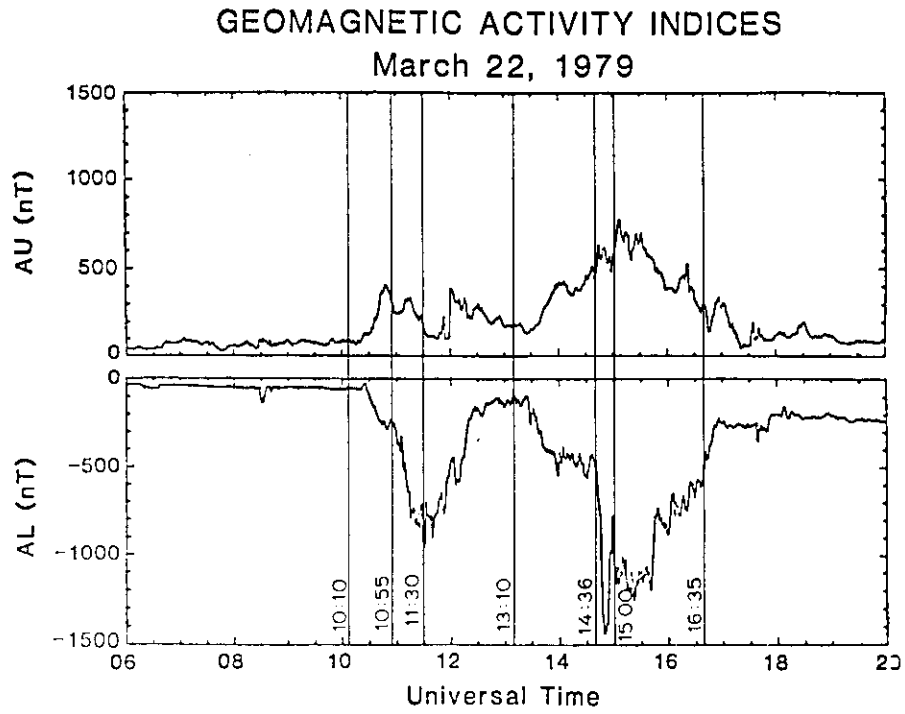
GEOMAGNETIC ACTIVITY INDICES
March 22, 1979
AU (nT)
AL (nT)
1500
1000
500
0
-500
-1000
-1500
10:10
10:55
11:30
13:10
14:36
15:00
16:35
06
08
10
12
14
16
18
20
Universal Time

Fig. 23

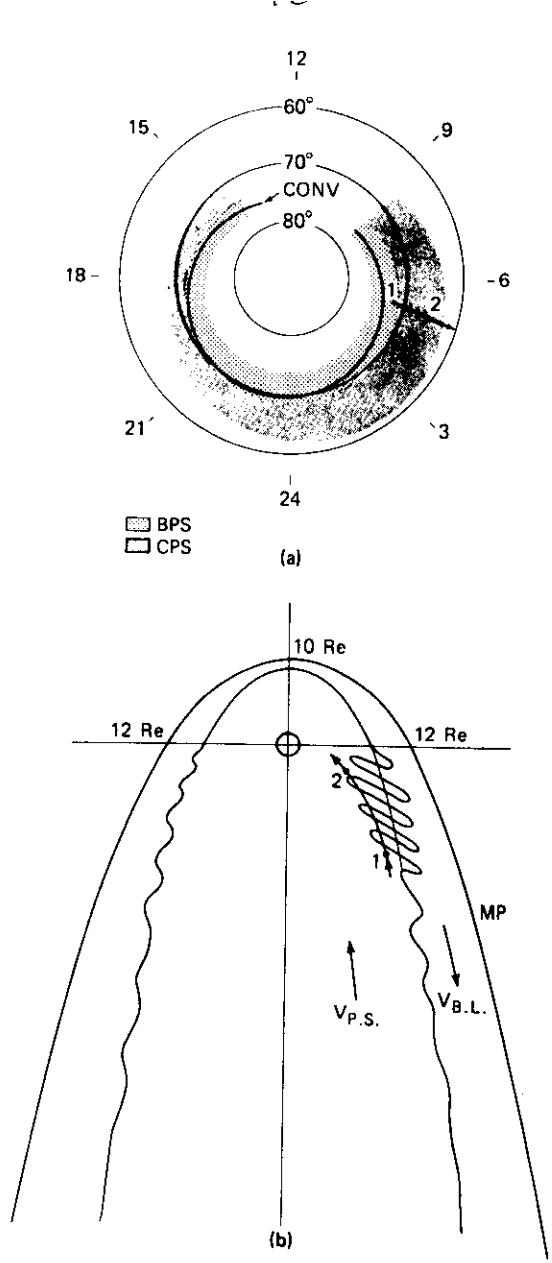
12
60°
15
9
70°
CONV
80°
18
-6
1
2
21
3
24
BPS
CPS
(a)
10 Re
12 Re
12 Re
2
1
MP
$V_{P.S.}$
$V_{B.L.}$
(b)

Fig. 24

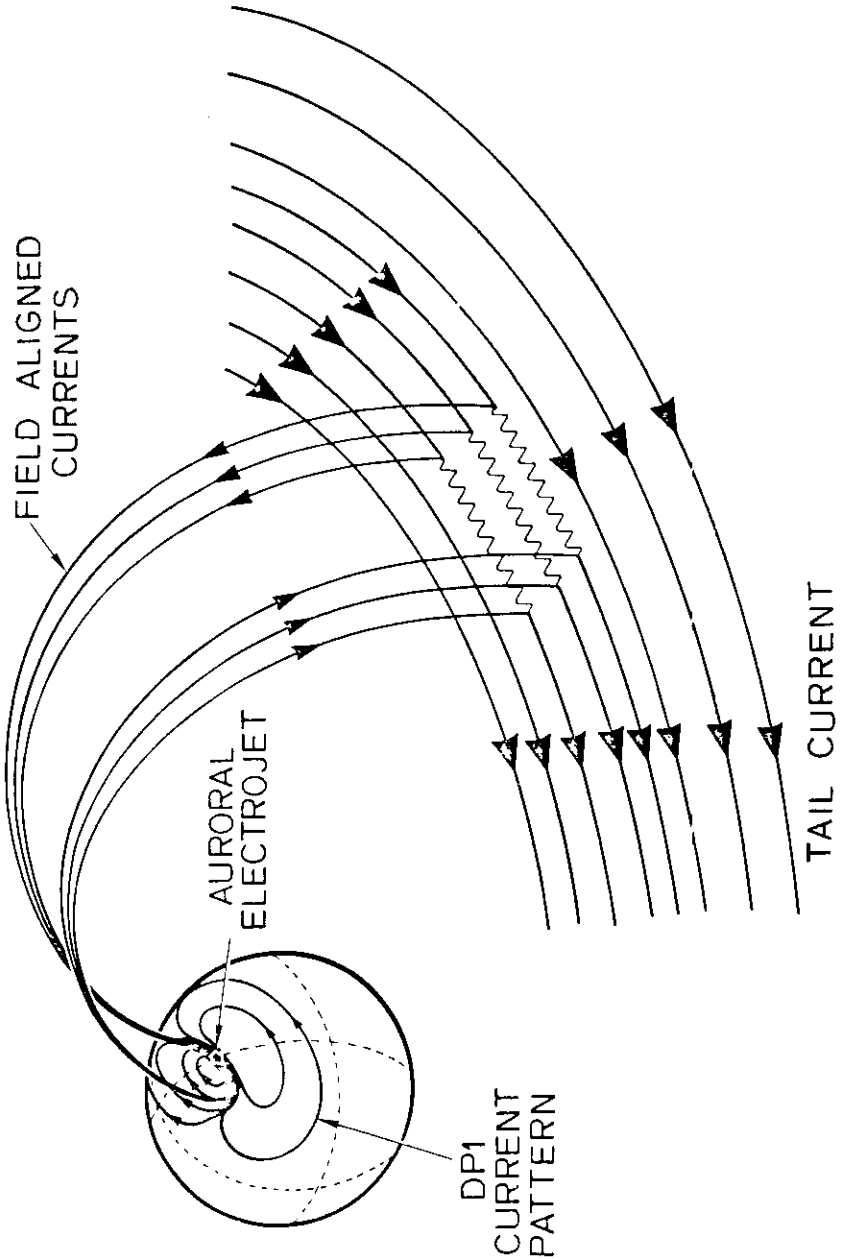

Fig. 25

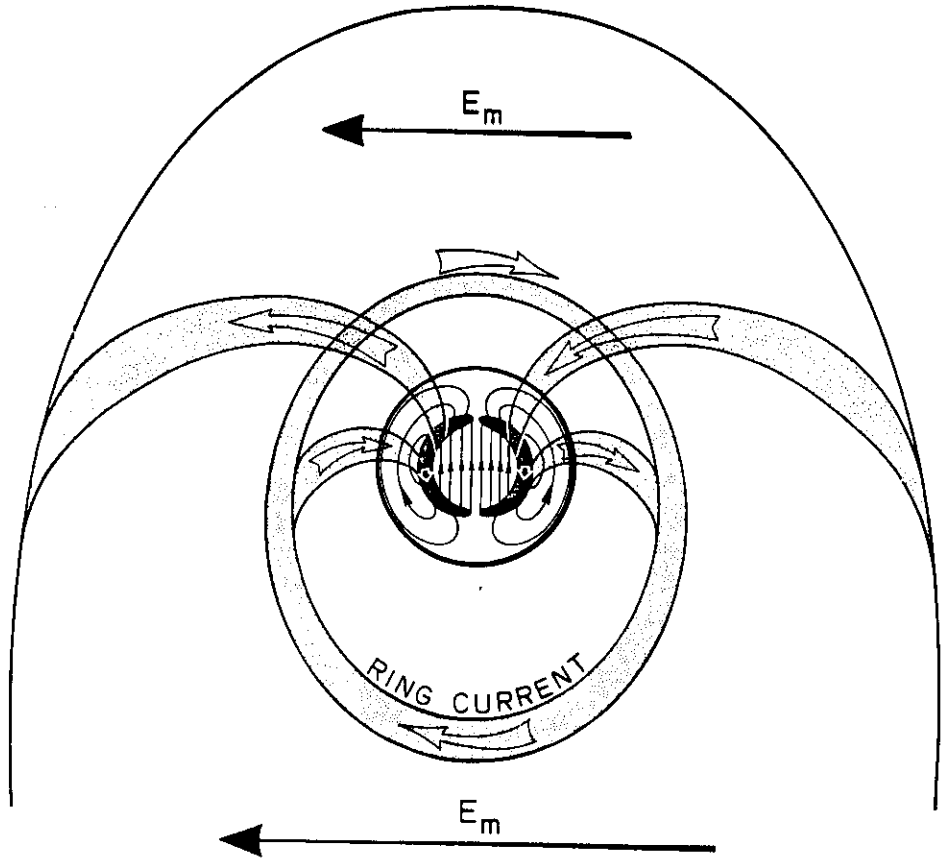

SOLAR WIND-MAGNETOSPHERE DYNAMO
AND DP2 EQUIVALENT CURRENT

Fig. 26

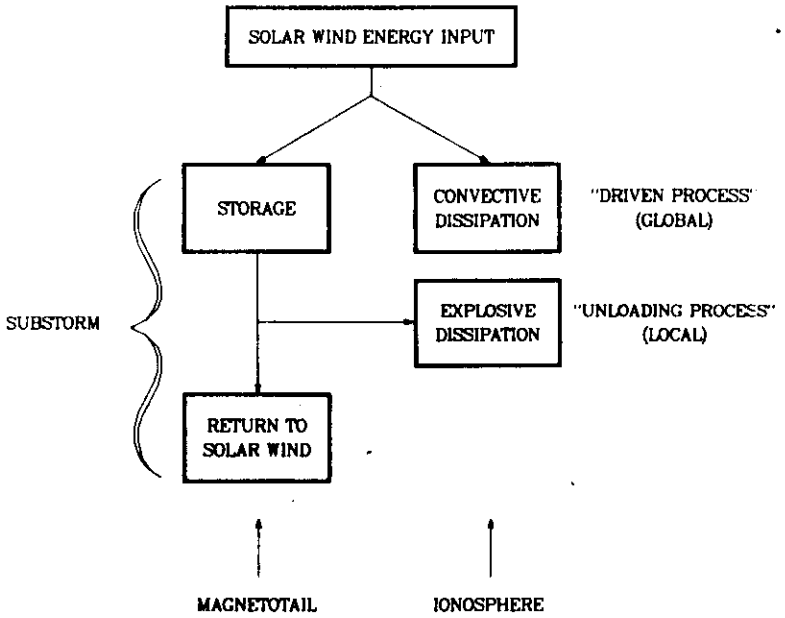

Fig. 27 A summary of the substorm sequence showing the roles of the magnetotail and the ionosphere and also showing the aspects of substorms which are regarded as driven and unloading processes (adapted from Baker et al., 1984).

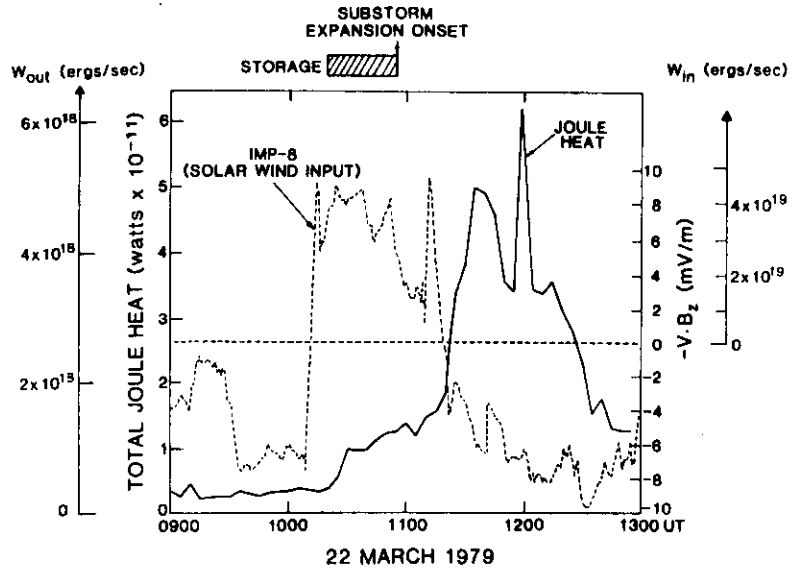

Fig. 28 A comparison of solar wind energy input to the magnetosphere (dashed line) compared to a measure of magnetospheric substorm energy output (Joule heat rate; solid line) for a particular event observed on 22 March 1979. The parameter $-VB_z$ is the dawn-to-dusk component of the solar wind electric field and is a measure of solar wind-magnetosphere coupling. W_{in} is positive for $-VB_z > 0$ and this energy input is estimated by the scale at the far right. W_{out} has several components but a major one is the Joule heating rate scaled to the far left.